Supplementary Material (ESI) for the paper

1D Co(II) coordination polymers based on cyclobutyl and cyclopentyl-substituted zoledronate analogues: synthesis, structural comparison, thermal stability and magnetic properties

Tomasz Rojek,*[a] Waldemar Goldeman,[a] Katarzyna Ślepokura[b], Marek Duczmal[a], Agnieszka Wojciechowska[a] and Ewa Matczak-Jon[a]

[a] Department of Chemistry, Wrocław University of Science and Technology, Wybrzeże Wyspiańskiego 27, 50-370 Wrocław, Poland. E-mail: tomasz.rojek@pwr.edu.pl

[b] Faculty of Chemistry, University of Wrocław, Joliot-Curie 14, 50-383 Wrocław, Poland.

Spectroscopic characterization of compounds **1** and **2**:

1-hydroxy-2-[1-(1*H*-imidazol-1-yl)cyclobutyl]ethylidene-1,1-diphosphonic acid (H_4cbtZol, **1**): ^{1}H NMR (300 MHz, D_2O+NaOD) δ: 1.35 (m, 2H, CH_2), 2.07 (m, 2H, CH_2), 2.86 (m, 2H, CH_2), 6.62 (s, 1H, imidazole-*H*), 7.40 (s, 1H, imidazole-*H*), 7.89 (s, 1H, 2-imidazole-*H*); ^{13}C NMR (75 MHz, D_2O+NaOD) δ: 15.57 (*C*H_2), 32.42 (t, $^3J_{CP}$ = 6.0 Hz, (*C*H_2)$_2$C), 68.85 ((CH$_2$)$_2$*C*), 78.31 (t, $^1J_{CP}$ = 126.8 Hz, P-*C*-P), 122.56, 124.26, 140.75; ^{31}P{^{1}H} NMR (121 MHz, D_2O+NaOD) δ: 17.37 (s, 2P).

1-hydroxy-2-[1-(1*H*-imidazol-1-yl)cyclopentyl]ethylidene-1,1-diphosphonic acid (H_4cptZol, **2**): ^{1}H NMR (300 MHz, D_2O+NaOD) δ: 0.88 (m, 2H, CH_2), 1.43 (m, 2H, CH_2), 2.19 (m, 2H, CH_2), 2.45 (m, 2H, CH_2), 6.60 (s, 1H, imidazole-*H*), 7.12 (s, 1H, imidazole-*H*), 7.61 (s, 1H, 2-imidazole-*H*); ^{13}C NMR (75 MHz, D_2O+NaOD) δ: 21.03 (*C*H_2), 35.22 ((*C*H_2)$_2$C), 74.96 (t, $^2J_{CP}$ = 4.5 Hz (CH$_2$)$_2$*C*), 79.45 (t, $^1J_{CP}$ = 124.5 Hz, P-*C*-P), 121.64, 124.64, 139.50; ^{31}P{^{1}H} NMR (121 MHz, D_2O+NaOD) δ: 17.49 (s, 2P).

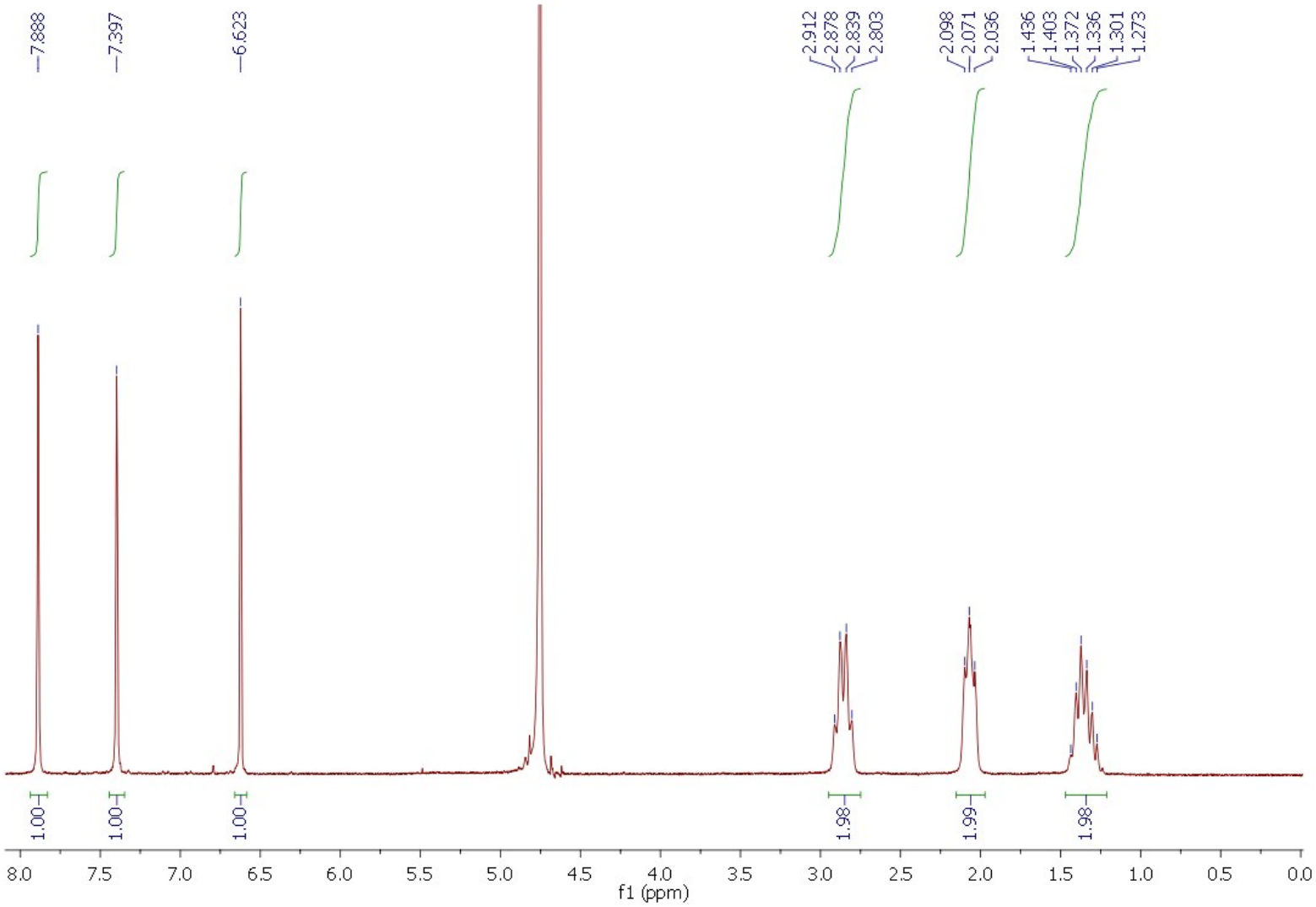

Figure S1. ^{1}H NMR spectrum of the compound **1**.

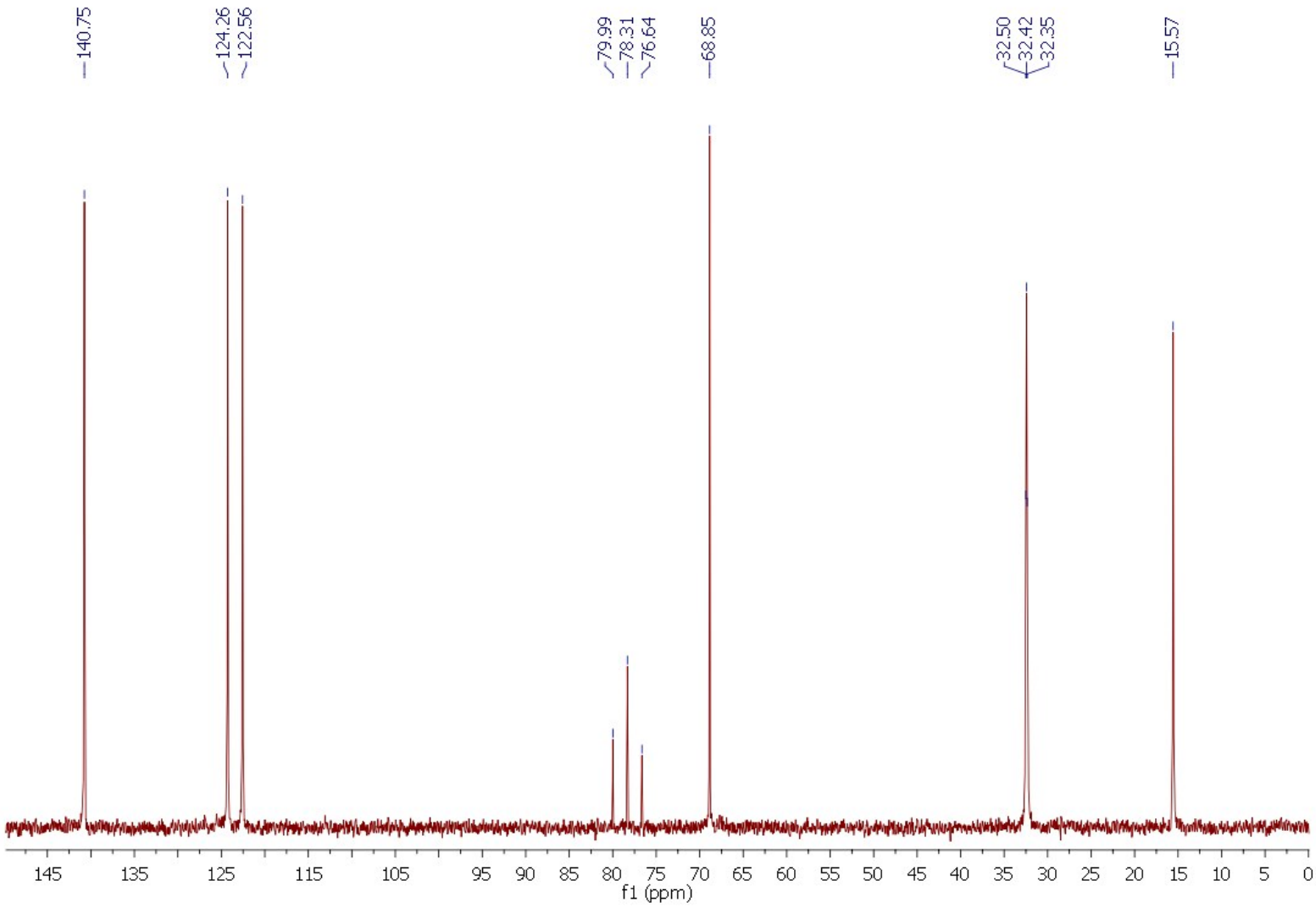

Figure S2. ^{13}C NMR spectrum of the compound **1**.

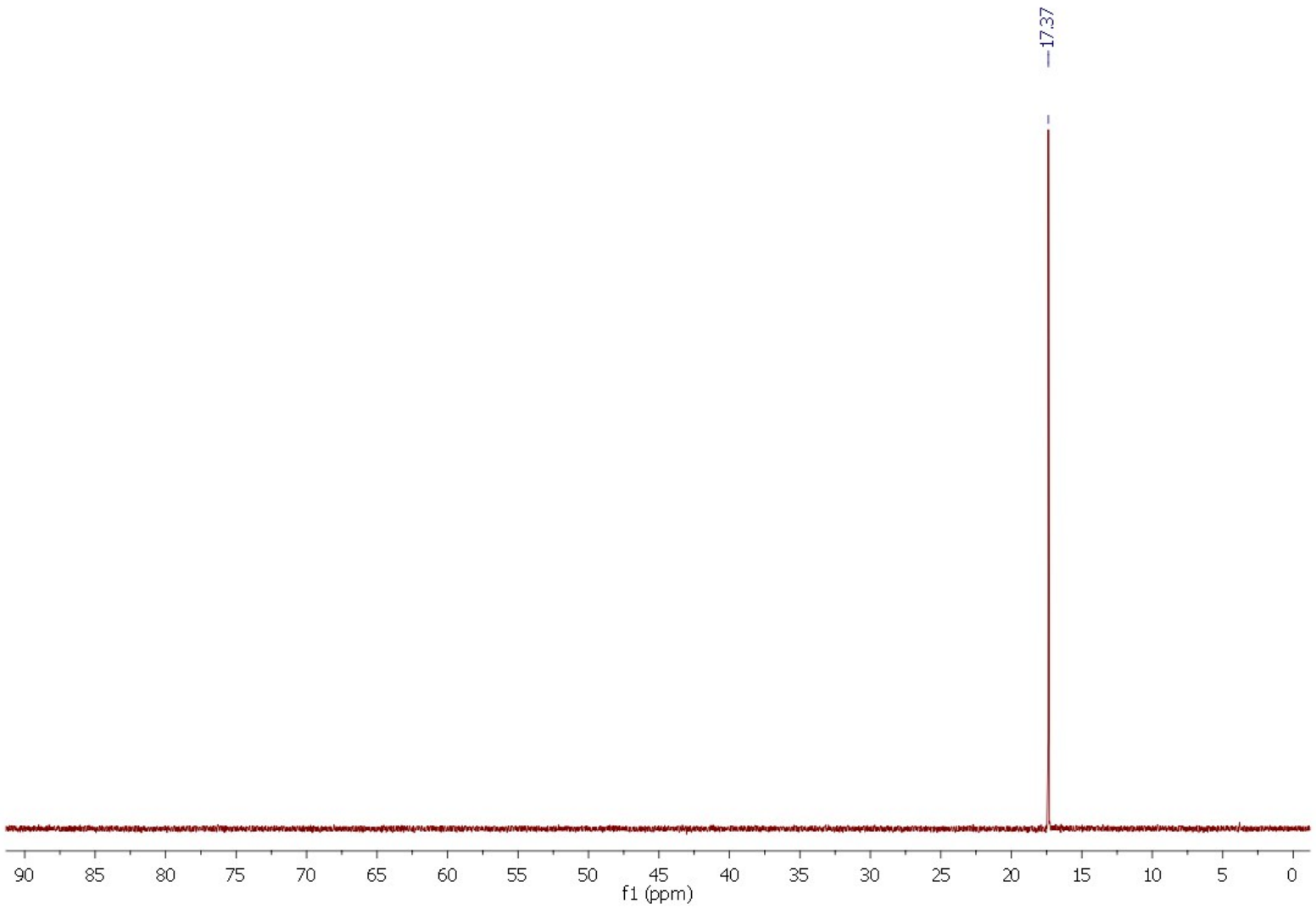

Figure S3. $^{31}P\{^{1}H\}$ NMR spectrum of the compound **1**.

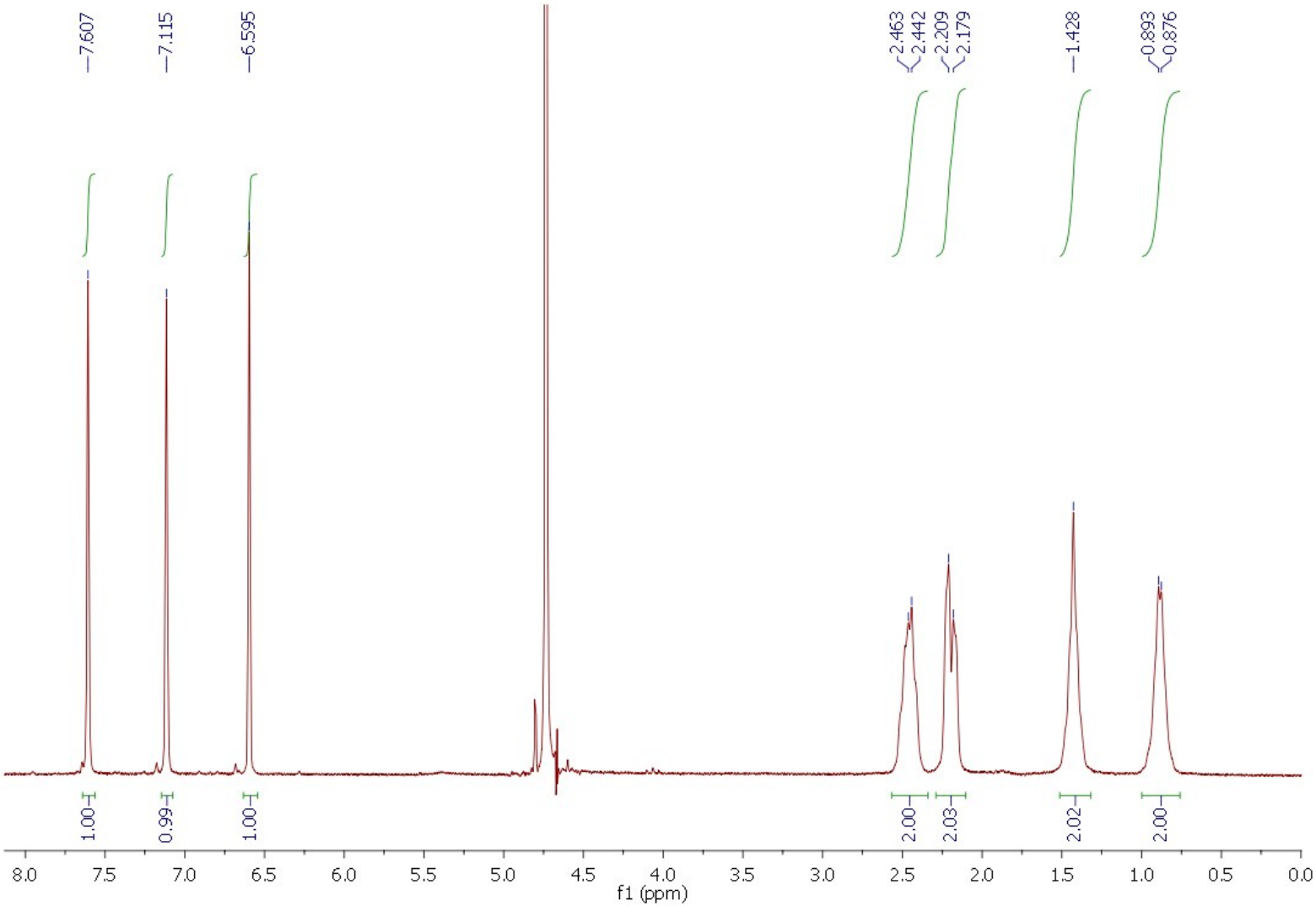

Figure S4. ^{1}H NMR spectrum of the compound **2**.

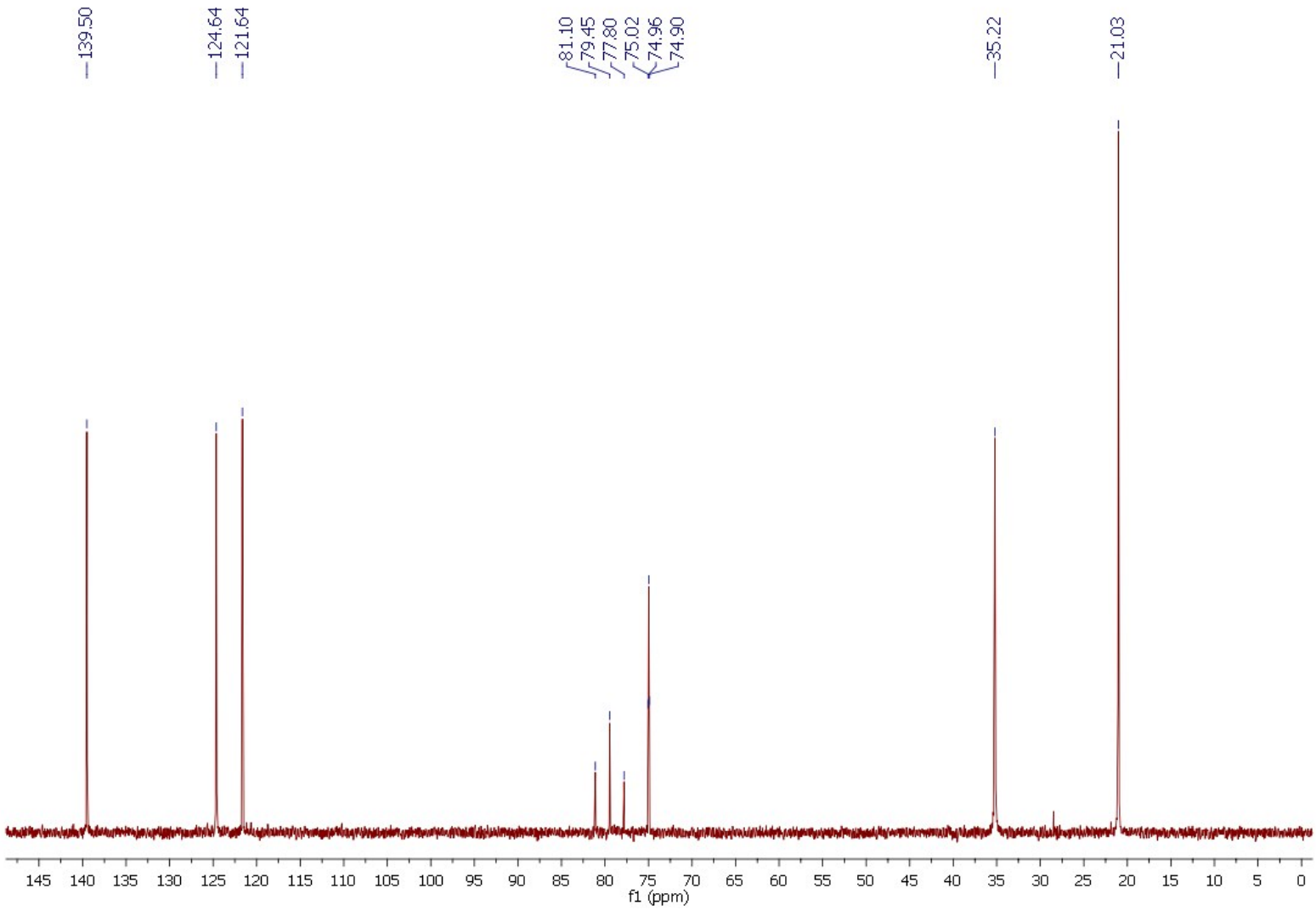

Figure S5. ^{13}C NMR spectrum of the compound **2**.

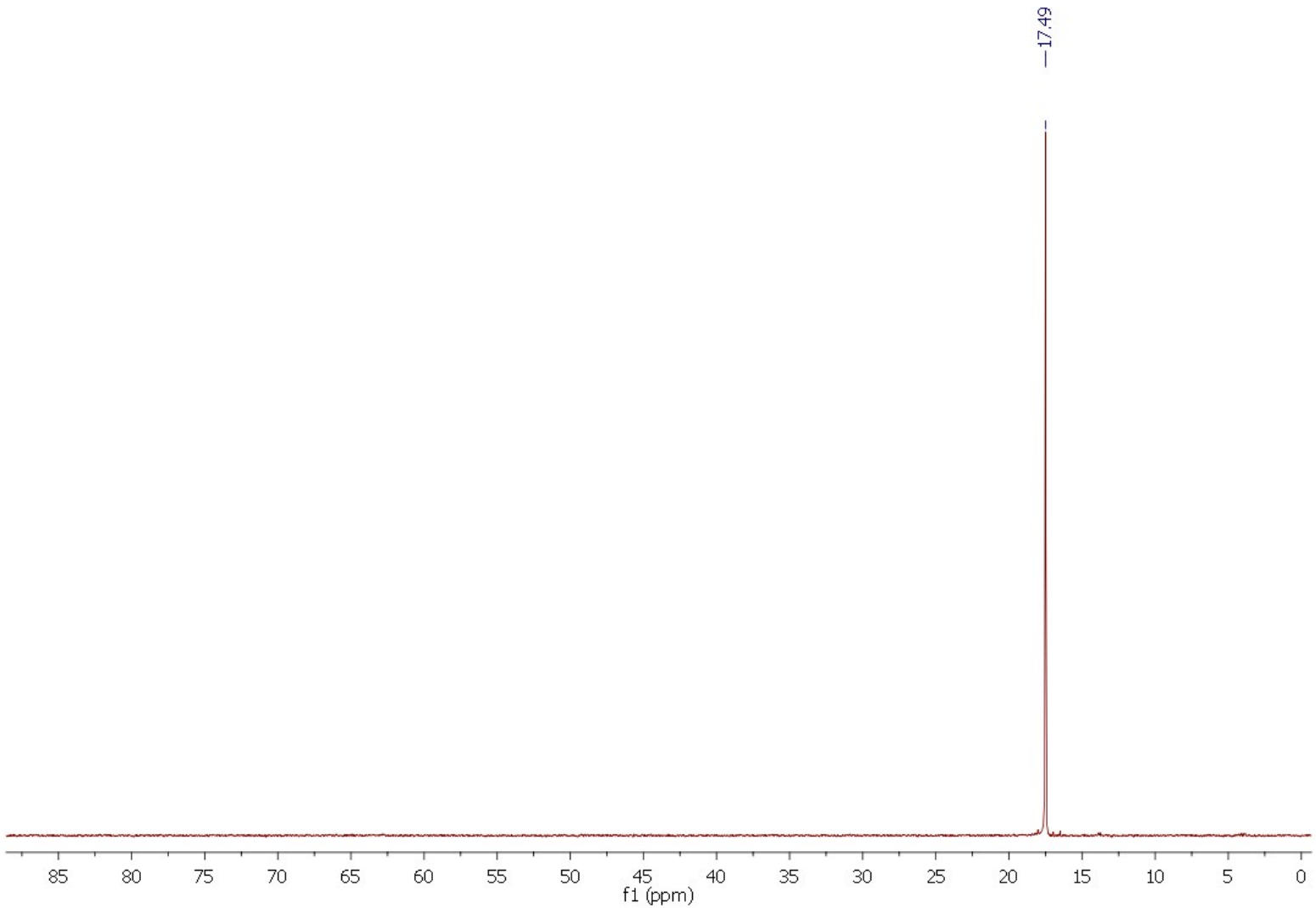

Figure S6. $^{31}P\{^{1}H\}$ NMR spectrum of the compound **2**.

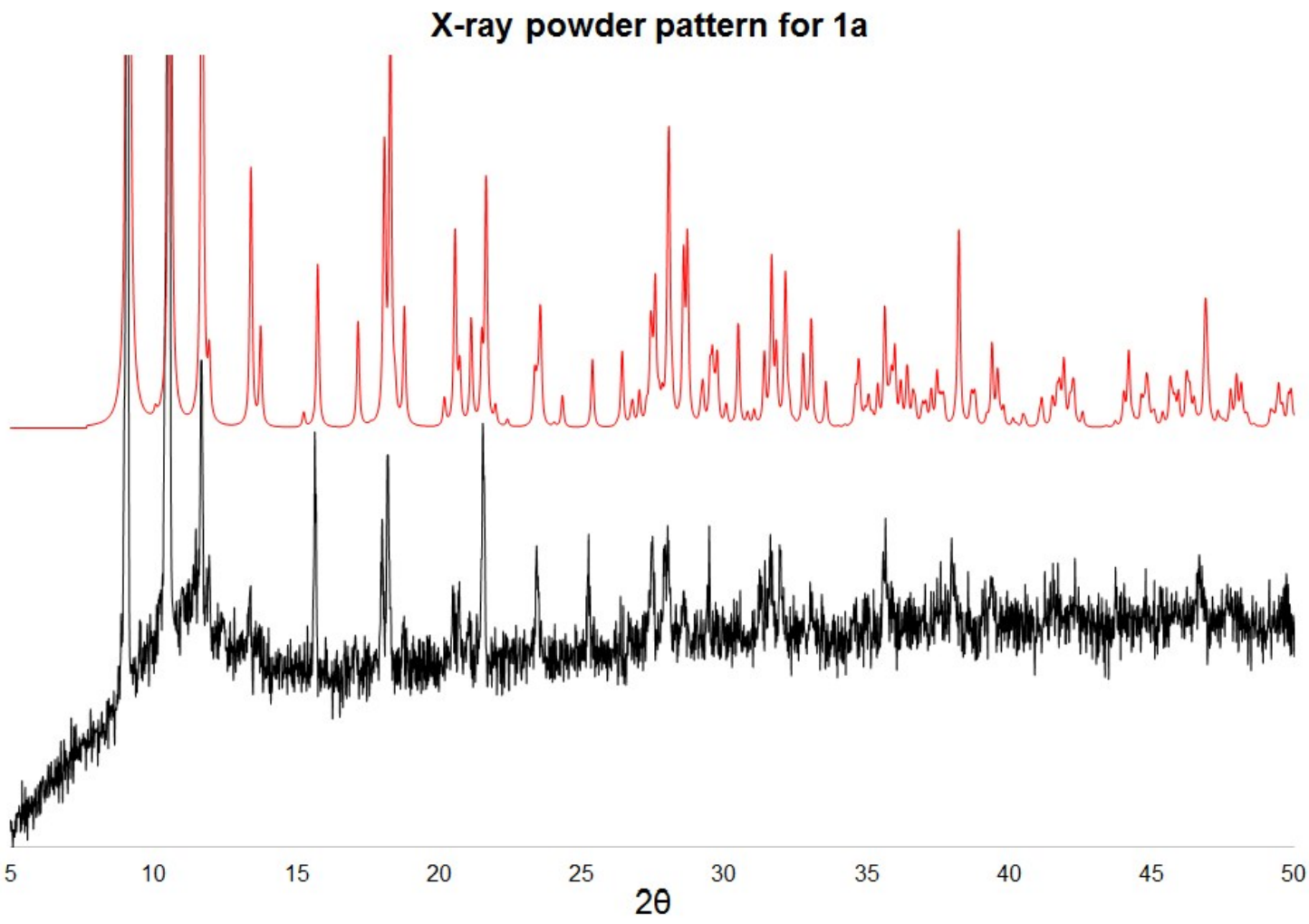

Figure S7. Experimental X-ray powder pattern (black, T = 298 K, Cu-Kα1) and simulated powder pattern (red, T = 80 K, Mo-Kα) based on the results from single-crystal X-ray diffraction for the coordination polymer **1a**.

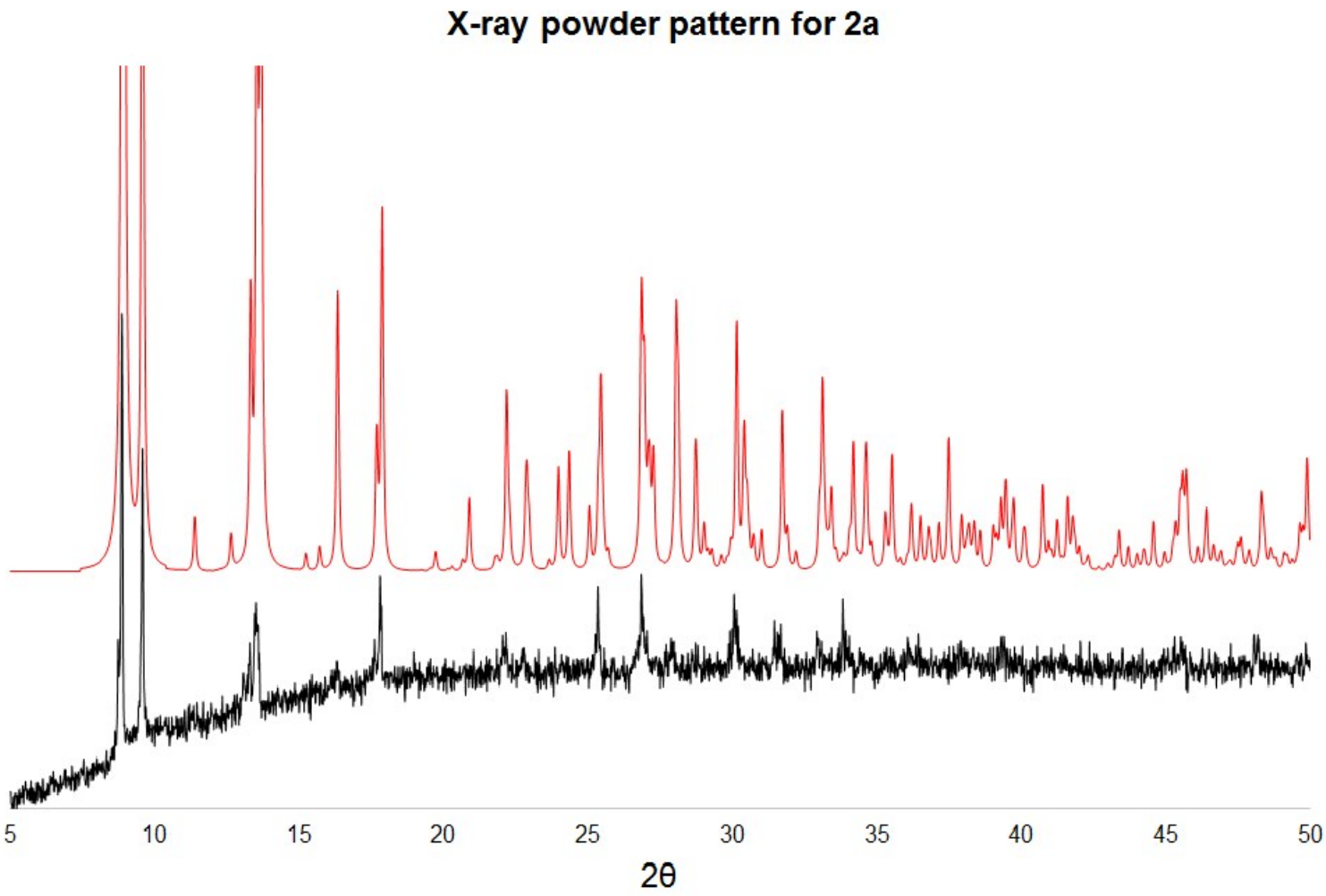

Figure S8. Experimental X-ray powder pattern (black, T = 298 K, Cu-Kα1) and simulated powder pattern (red, T = 130 K, Mo-Kα) based on the results from single-crystal X-ray diffraction for the coordination polymer **2a**.

Table S1. Coordination modes of zoledronic acid (H_4Zol) and its derivatives (H_4dmtZol and H_4cppZol) in known metal complexes of 3:2 molar ratio with various metal ions (without auxiliary ligands).

	Database refcode	*Formula*	*Dimensionality*	*Coordination mode*	*Source*
Zoledronic acid (H_4Zol)					
Co					
1.	OXAMOQ	$Co_3(HZol)_2(H_2O)_4$	2D	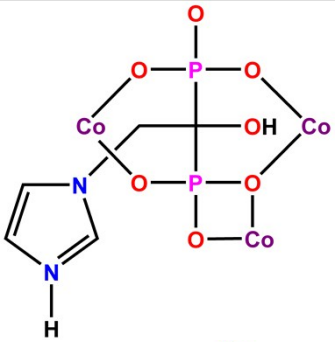	Cao *et al.*, *Inorg. Chem.*, **50** (2011) 2278–2287
2.	VIMXEV	α-$Co_3(HZol)_2(H_2O)_4 \cdot 2H_2O$	2D	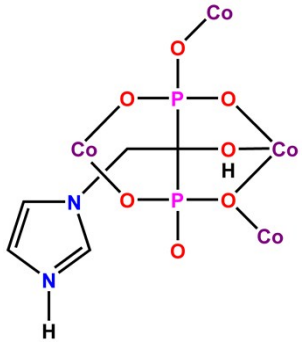	Cao *et al.*, *Inorg. Chem.*, **46** (2007) 7571–7578

3.	OXAMIK	β-$Co_3(HZol)_2(H_2O)_4 \cdot 2H_2O$	3D	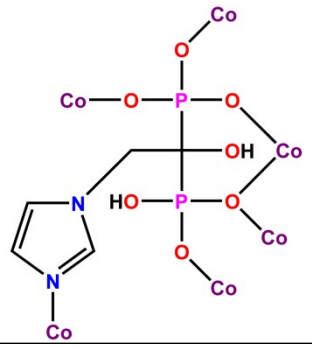	Cao *et al.*, *Inorg. Chem.*, **50** (2011) 2278–2287
Ni					
4.	VIMXIZ	$Ni_3(HZol)_2(H_2O)_4 \cdot 2H_2O$	2D	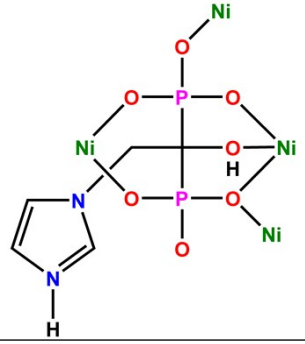	Cao *et al.*, *Inorg. Chem.*, **46** (2007) 7571–7578
Cu					
5.	GOZPUI	$Cu_3(HZol)_2(H_2O)_6 \cdot 6H_2O$	1D	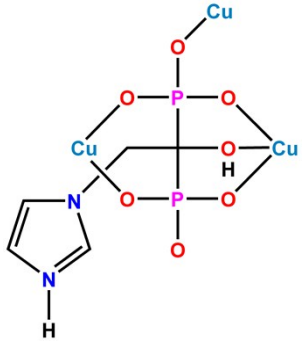	Qiu *et al.*, *Eur. J. Med. Chem.*, **89** (2015) 42–50

6.	DOGYUU	$Cu_3(HZol)_2 \cdot 2H_2O$	2D	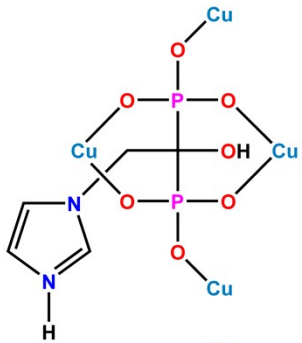	Cao *et al.*, *Dalton Trans.*, **37** (2008) 5008-5015
7.	DOGYUU01	$Cu_3(HZol)_2(H_2O)_2$	2D	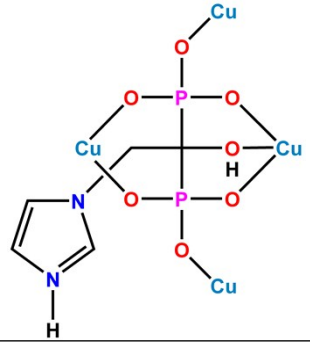	Li *et al.*, *Acta Cryst.*, E**66** (2010) m1576
Zn					
8.	VIRXEB	$Zn_3(HZol)_2(H_2O)_4$	2D	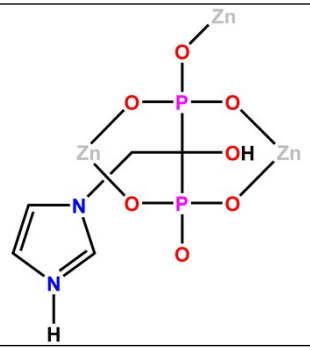	Zhang *et al.*, *Dalton Trans.*, **43** (2014) 285–289

Dimethyl derivative of zoledronic acid (H_4dmtZol)					
Co					
9.	HARGEP	$Co_3(HdmtZol)_2(H_2O)_6 \cdot 6H_2O$	1D	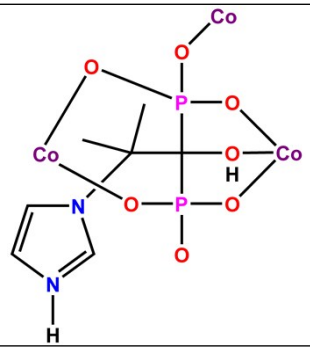	Rojek *et al*., *Dalton Trans.*, **46** (2017) 6900-6911
Ni					
10.	KEQVOU	$Ni_3(HdmtZol)_2(H_2O)_6 \cdot 6H_2O$	1D	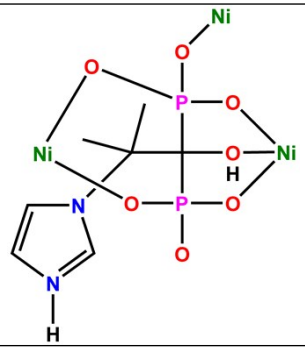	Rojek *et al*., *Polyhedron*, **141** (2018) 44-51

Cyclopropyl derivative of zoledronic acid (H_4cppZol)					
Co					
11.	HARGIT	$Co_3(HcppZol)_2(H_2O)_6 \cdot 6H_2O$	1D	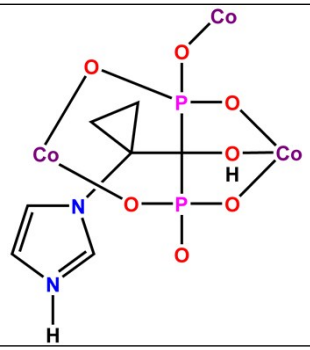	Rojek *et al*., *Dalton Trans.*, **46** (2017) 6900-6911

Table S2. Selected interatomic distances (Å), bond angles (°) and torsion angles (°) for the compounds **1**, **1a**, **2** and **2a**.

	1	**1a**	**2**	**2a**
Bond lenghts				
P1–O1	1.4951(10)	1.498(2)	1.4950(16)	1.499(2)
P1–O2	1.5463(11)	1.524(2)	1.5133(16)	1.529(2)
P1–O3	1.5505(10)	1.547(2)	1.5643(16)	1.542(2)
P2–O4	1.5060(11)	1.512(2)	1.4955(16)	1.5058(19)
P2–O5	1.5192(10)	1.516(2)	1.5489(18)	1.528(2)
P2–O6	1.5633(11)	1.540(2)	1.5499(17)	1.539(2)
Bond angles				
N1–C2–C1	107.93(8)	110.2(2)	107.59(16)	111.1(2)
O1–P1–O2	109.39(6)	112.50(13)	116.15(10)	114.24(12)
O1–P1–O3	112.68(6)	112.11(13)	111.85(9)	111.93(11)
O2–P1–O3	109.76(6)	111.78(13)	106.88(9)	110.45(11)
O4–P2–O5	115.28(6)	110.58(13)	114.59(9)	112.02(12)
O4–P2–O6	111.67(6)	111.93(13)	112.94(9)	112.68(12)
O5–P2–O6	108.39(6)	112.90(13)	104.76(9)	110.54(11)
Torsion angles				
O7–C1–C2–N1	-65.15(11)	-60.6(3)	-71.03(19)	-79.1(3)
P1–C1–C2–N1	54.34(11)	55.2(3)	47.48(19)	35.0(3)
P2–C1–C2–N1	179.81(8)	-177.22(19)	172.63(13)	163.49(17)
O7–C1–C2–C5	164.06(9)	169.0(2)	-	-
P1–C1–C2–C5	-76.45(11)	-75.2(3)	-	-
P2–C1–C2–C5	49.02(13)	52.4(3)	-	-
O7–C1–C2–C6	-	-	165.59(17)	157.2(2)
P1–C1–C2–C6	-	-	-75.9(2)	-88.8(2)
P2–C1–C2–C6	-	-	49.2(2)	39.7(3)
O7–C1–C2–C3	59.67(11)	65.7(3)	46.6(2)	40.4(3)
P1–C1–C2–C3	179.16(7)	-178.6(2)	165.12(14)	154.47(18)
P2–C1–C2–C3	-55.37(12)	-50.9(3)	-69.7(2)	-77.0(2)

Table S3. Proposed hydrogen bonds for **1** and **2**.

D—H···*A*	*D*—H	H···*A*	*D*···*A*	*D*—H···*A*
*Compound **1***				
O2–H2···O1*W*	0.84	1.71	2.5211(14)	161
O3–H3···O5	0.84	1.68	2.5064(16)	166
O6–H6···O4^{i}	0.84	1.72	2.5553(15)	170
O7–H7···O1^{ii}	0.84	1.88	2.6882(16)	162
N2–H2*N*···O1^{iii}	0.88	1.85	2.7271(17)	173
O1*W*–H1*W*···O5^{iv}	0.84	1.97	2.7723(15)	160
O1*W*–H2*W*···O4	0.84	1.91	2.6876(17)	153
C3–H3*B*···O6	0.99	2.39	3.1262(18)	131
C5–H5*A*···O4	0.99	2.46	3.1476(18)	126
C21–H21···O5^{v}	0.95	2.25	3.116(2)	152
*Compound **2***				
O3–H3···O4*W*	0.84	1.70	2.534(3)	173
O5–H5···O1*W*	0.84	1.78	2.530(2)	148
O6–H6···O2^{vi}	0.84	1.72	2.519(2)	158
O7–H7···O3*W*^{vii}	0.84	2.04	2.803(2)	151
N2–H2*N*···O2^{viii}	0.88	1.87	2.740(3)	169
O1*W*–H1*W*···O2*W*	0.84	1.95	2.772(3)	167
O1*W*–H2*W*···O1^{ix}	0.84	1.84	2.658(2)	164
O2*W*–H3*W*···O4^{v}	0.84	1.94	2.772(2)	173
O2*W*–H4*W*···O1*W*^{x}	0.84	2.08	2.873(3)	156
O3*W*–H5*W*···O1^{ix}	0.84	1.93	2.753(2)	167
O3*W*–H6*W*···O2*W*	0.84	1.98	2.787(3)	161
O4*W*–H7*W*···O3*W*^{vii}	0.84	1.88	2.677(3)	159
O4*W*–H8*W*···O4^{xi}	0.84	1.93	2.737(3)	160
C3–H3*B*···O4	0.99	2.37	3.141(3)	134
C51–H51···O4^{v}	0.95	2.50	3.441(3)	173

Symmetry codes:
(i) −*x*, −*y*+1, −*z*+1; (ii) −*x*, −*y*, −*z*; (iii) −*x*+1, −*y*, −*z*; (iv) −*x*, −*y*, −*z*+1;
(v) *x*+1, *y*, *z*; (vi) *x*−1, *y*, *z*; (vii) *x*−1, −*y*+1/2, *z*−1/2;
(viii) *x*, −*y*+1/2, *z*−1/2; (ix) *x*, −*y*+1/2, *z*+1/2; (x) −*x*+1, −*y*+1, −*z*+1;
(xi) −*x*, *y*−1/2, −*z*+1/2

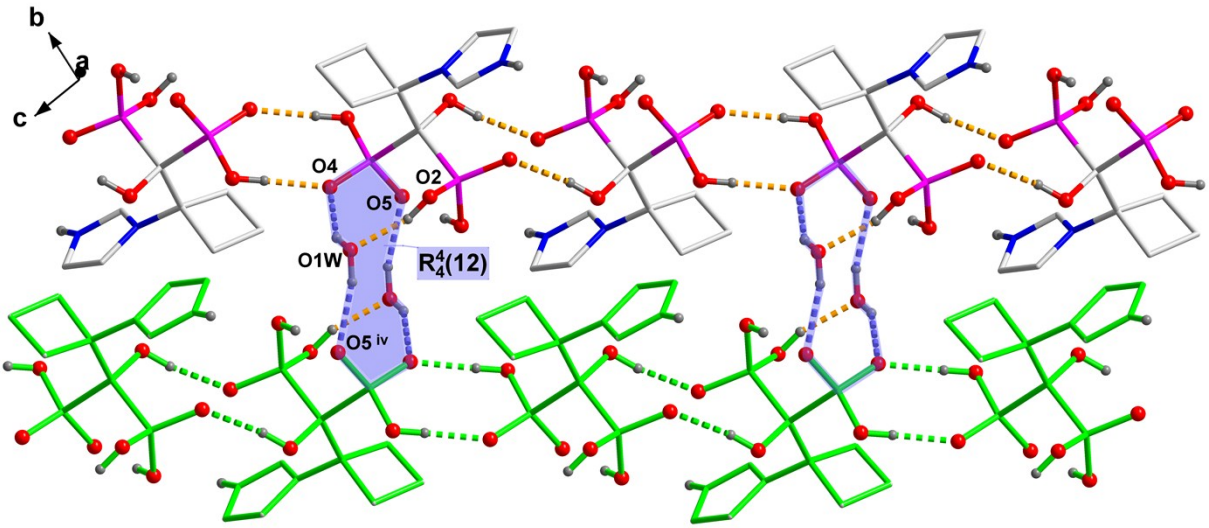

Figure S9. Interconnection of two-dimensional layers (shown in two-colored and bright green sticks) into three-dimensional hydrogen-bonded network. All C-bounded H-atoms are omitted for clarity. Symmetry codes are given in Table S3.

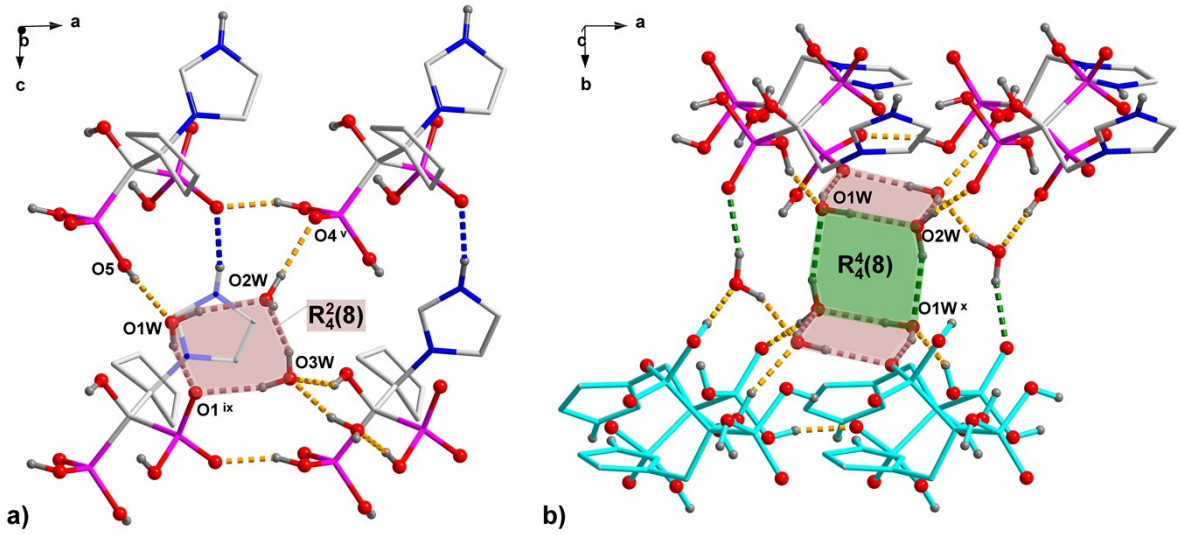

Figure S10. (a) Role of lattice water molecules in stabilizing the two-dimensional layer and (b) interconnecting the two neighboring layers (shown in two-colored and turquoise sticks) into three-dimensional supramolecular network. All O–H···O hydrogen bonds within a single layer (except those that are a part of the eight-member ring) and joining adjacent layers are shown as dashed lines (orange and green, respectively). N–H···O type hydrogen bonds are

indicated as blue dashed lines. All C-bounded H-atoms and cyclopentane rings (picture b) are omitted for clarity. Symmetry codes are given in Table S3.

Table S4. Selected interatomic distances (Å) and bond angles (°) for the compounds **1a** and **2a**.

*Compound **1a***			
Bond lengths (Å)			
Co1–O2, O2^{i}	2.077(2)	Co2–O3	2.039(2)
Co1–O5, O5^{i}	2.035(2)	Co2–O4^{ii}	2.007(2)
Co1–O1*W*, O1*W*^{i}	2.186(2)	Co2–O6	2.143(2)
		Co2–O7	2.226(2)
		Co2–O2*W*	2.136(2)
		Co2–O3*W*	2.084(2)
Bond angles (°)			
O2–Co1–O1*W*	87.38(9)	O3–Co2–O3*W*	93.65(10)
O2–Co1–O1*W*^{i}	92.62(9)	O4^{ii}–Co2–O6	89.94(9)
O5–Co1–O2	90.06(9)	O4^{ii}–Co2–O7	92.43(9)
O5^{i}–Co1–O2	89.94(9)	O4^{ii}–Co2–O2*W*	89.80(10)
O5–Co1–O1*W*	90.00(10)	O4^{ii}–Co2–O3*W*	90.32(10)
O5–Co1–O1*W*^{i}	90.00(10)	O6–Co2–O7	79.70(8)
O3–Co2–O6	85.83(9)	O2*W*–Co2–O6	100.57(9)
O3–Co2–O7	85.52(9)	O2*W*–Co2–O3*W*	88.55(11)
O3–Co2–O2*W*	92.28(10)	O3*W*–Co2–O7	91.18(10)
*Compound **2a***			
Bond lengths (Å)			
Co1–O2, O2^{ii}	2.092(2)	Co2–O3	2.050(2)
Co1–O5, O5^{ii}	2.026(2)	Co2–O3^{iii}	2.089(2)
Co1–O1*W*, O1*W*^{ii}	2.273(2)	Co2–O6	2.050(2)
		Co2–O7	2.247(2)
		Co2–O1*W*^{iii}	2.163(2)
		Co2–O2*W*	1.988(2)
Bond angles (°)			
O2–Co1–O1*W*	98.85(8)	O3–Co2–O1*W*^{iii}	84.46(8)
O2–Co1–O1*W*^{ii}	81.16(8)	O3^{iii}–Co2–O1*W*^{iii}	82.38(8)
O5–Co1–O2	89.22(9)	O6–Co2–O3^{iii}	89.22(8)
O5^{ii}–Co1–O2	90.78(9)	O6–Co2–O7	81.95(8)
O5–Co1–O1*W*	88.19(9)	O1*W*^{iii}–Co2–O7	104.04(8)
O5–Co1–O1*W*^{ii}	91.81(9)	O2*W*–Co2–O6	103.27(8)
O3–Co2–O6	87.09(8)	O2*W*–Co2–O7	89.00(8)
O3–Co2–O7	81.24(8)	O2*W*–Co2–O3^{iii}	107.97(9)
O3–Co2–O3^{iii}	83.07(9)	O2*W*–Co2–O1*W*^{iii}	86.54(8)

Symmetry codes: (i) −*x*+2, −*y*, −*z*+1; (ii) −*x*+1, −*y*+1, −*z*+1; (iii) –*x*, −*y*+1, −*z*+1.

Table S5. Proposed hydrogen bonds for **1a** and **2a**.

D—H···*A*	*D*—H	H···*A*	*D*···*A*	*D*—H···*A*
*Compound **1a***				
O7–H7*O*···O6^{ii}	0.84	1.96	2.778(3)	166
N2–H2*N*···O2^{v}	0.88	1.85	2.719(4)	169
O1*W*–H1*W*···O3	0.84	1.98	2.767(3)	156
O1*W*–H2*W*···O5*W*	0.84	1.95	2.702(5)	149
O2*W*–H3*W*···O3^{iv}	0.84	1.98	2.798(3)	163
O3*W*–H5*W*···O6*W*	0.84	1.94	2.717(4)	154
O3*W*–H6*W*···O4*W*	0.84	1.88	2.639(5)	150
O4*W*–H8*W*···O1	0.84	1.82	2.616(6)	157
O5*W*–H10*W*···O6	0.84	1.99	2.780(5)	157
O6*W*–H11*W*···O5^{vi}	0.84	1.89	2.727(3)	171
O6*W*–H12*W*···O2*W*	0.84	2.38	2.962(4)	127
C3–H3*B*···O2*W*^{ii}	0.99	2.46	3.259(4)	137
C5–H5*A*···O1*W*^{i}	0.99	2.46	3.392(4)	157
C21–H21···O1^{v}	0.95	2.33	3.052(4)	133
*Compound **2a***				
O7–H7···O4^{vii}	0.84	1.91	2.701(3)	156
N2–H2*N*···O2^{viii}	0.88	1.88	2.753(3)	170
O1*W*–H1*W*···O6	0.84	1.86	2.680(3)	165
O1*W*–H2*W*···O3*W*^{iii}	0.84	1.98	2.774(3)	159
O2*W*–H3*W*···O5^{vi}	0.84	1.82	2.645(3)	167
O2*W*–H4*W*···O4^{vii}	0.84	1.86	2.637(3)	154
O3*W*–H5*W*···O1^{ix}	0.84	1.95	2.789(3)	174
O3*W*–H6*W*···O1	0.84	2.16	2.985(3)	167
C3–H3*A*···O4	0.99	2.43	3.187(3)	133
C3–H3*A*···O6^{vii}	0.99	2.46	3.162(4)	128
C3–H3*A*···O2*W*^{vii}	0.99	2.56	3.223(4)	124
C6–H6*B*···O5	0.99	2.51	3.195(3)	126
C21–H21···O3*W*^{x}	0.95	2.48	3.432(4)	177
C41–H41···O6^{xi}	0.95	2.35	3.242(3)	157

Symmetry codes: (i) −*x*+2, −*y*, −*z*+1; (ii) −*x*+1, −*y*+1, −*z*+1; (iii) −*x*, −*y*+1, −*z*+1; (iv) −*x*+1, −*y*, −*z*+1; (v) −*x*+2, −*y*, −*z*; (vi) *x*−1, *y*, *z*; (vii) −*x*, −*y*, −*z*+1; (viii) −*x*+1, −*y*+1, −*z*+2; (ix) −*x*, −*y*+1, −*z*+2; (x) *x*+1, *y*, *z*.

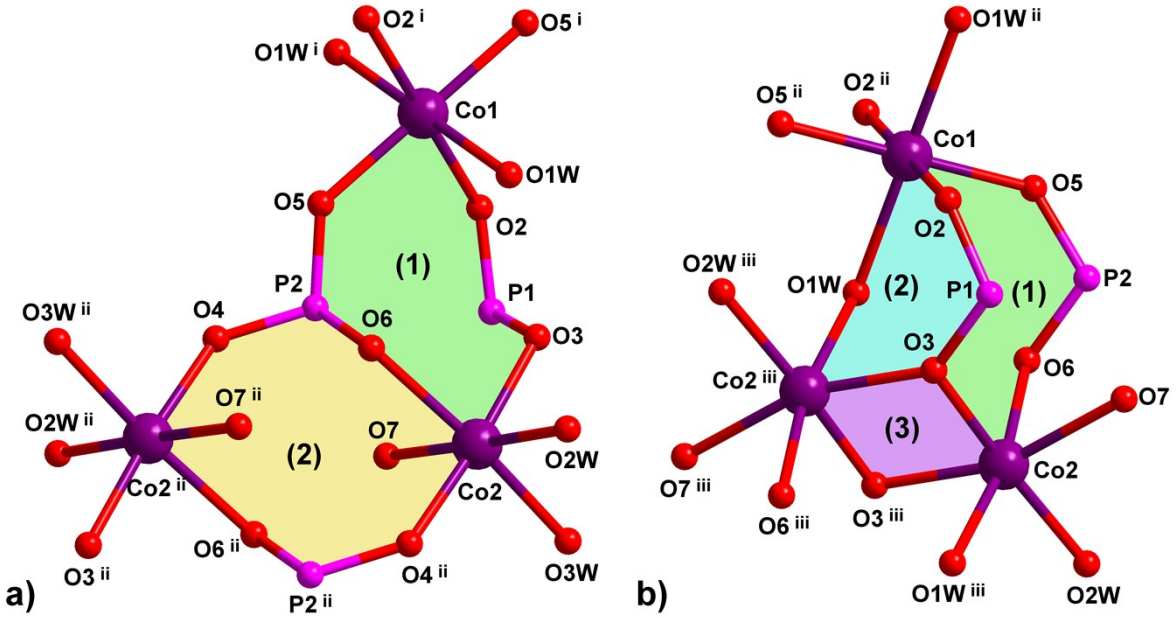

Figure S11. Connection of Co(II) ions leading to the formation of (a) two 8-member rings (1 and 2) in **1a** with Co1···Co2 and Co2···Co2^{ii} distances which are 5.012(2) Å and 4.804(2) Å, respectively; (b) 8-, 6- and 4-member rings (1, 2 and 3, respectively) in **2a** with Co1···Co2, Co1···Co2^{iii} and Co2···Co2^{iii} distances which are 4.715(2) Å, 3.781(2) Å and 3.098(2) Å, respectively. Symmetry codes: (i) −*x*+2, −*y*, −*z*+1; (ii) −*x*+1, −*y*+1, −*z*+1; (iii) –*x*, −*y*+1, −*z*+1.

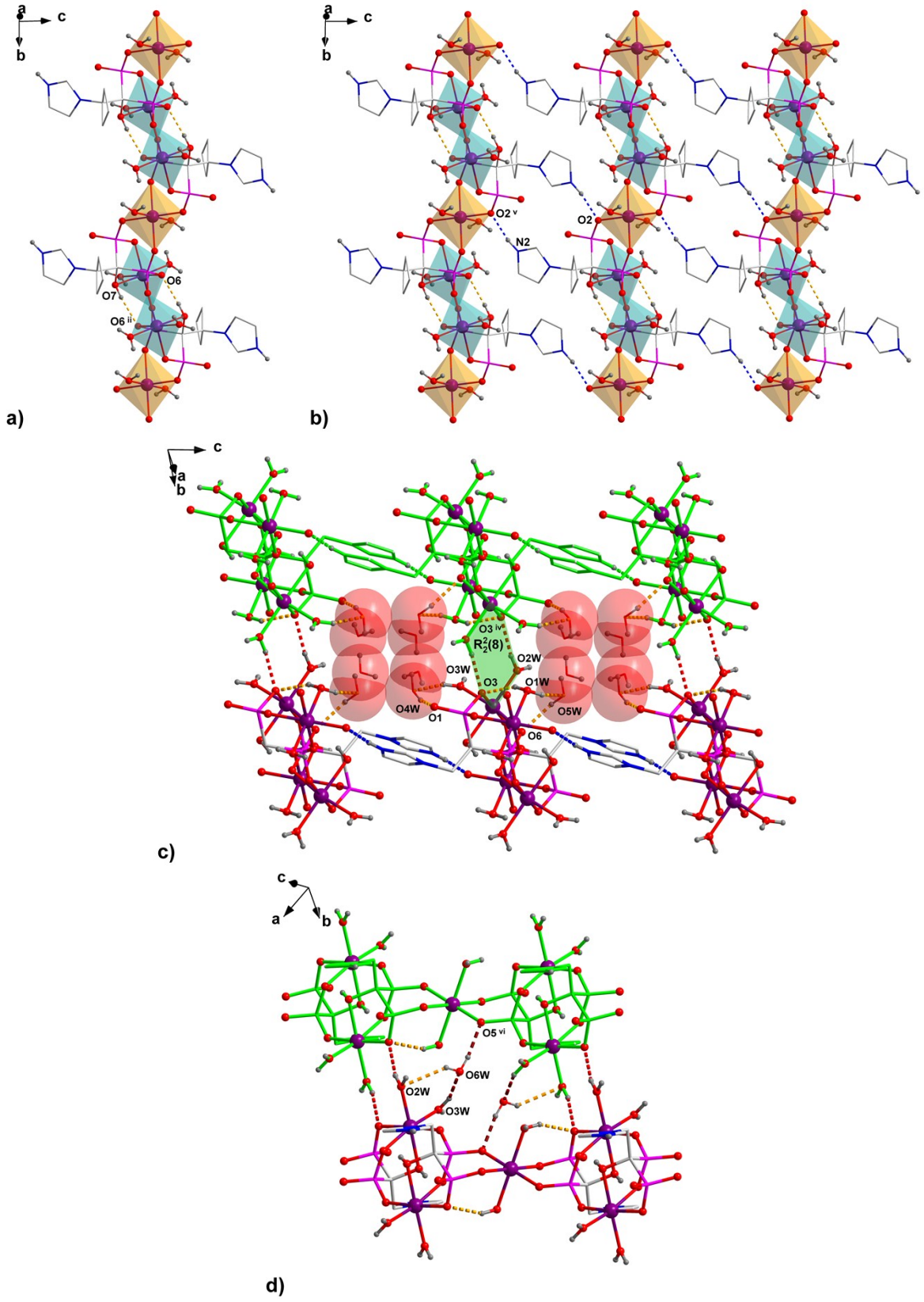

Figure S12. A packing diagram for $Co_3(HcbtZol)_2(H_2O)_6 \cdot 6H_2O$ coordination polymer (**1a**). (a) 1D infinite coordination chains stabilized by intrachain O–H···O type hydrogen bonds

(shown as orange dashed lines). (b) Formation of 2D layer parallel to (110) crystallographic plane by means of N–H···O type hydrogen bonds (shown as blue dashed lines). (c) Role of coordinated and lattice water molecules in connection of adjacent layers (shown as two-colored and bright green sticks) into 3D supramolecular hydrogen bonded network. (d) Additional stabilization of the network provided by O6*W* lattice water molecules. Hydrogen bonds within and between the layers are shown as orange and red dashed lines, respectively. All C-bound H-atoms, cyclobutane rings (pictures c and d), lattice water molecules (picture a and b) and O6*W* lattice water molecule (pictures a,b and c) are omitted for clarity. Disordered O4*W* and O5*W* water molecules are shown as space-filling models (picture c). Symmetry codes are given in Table S5.

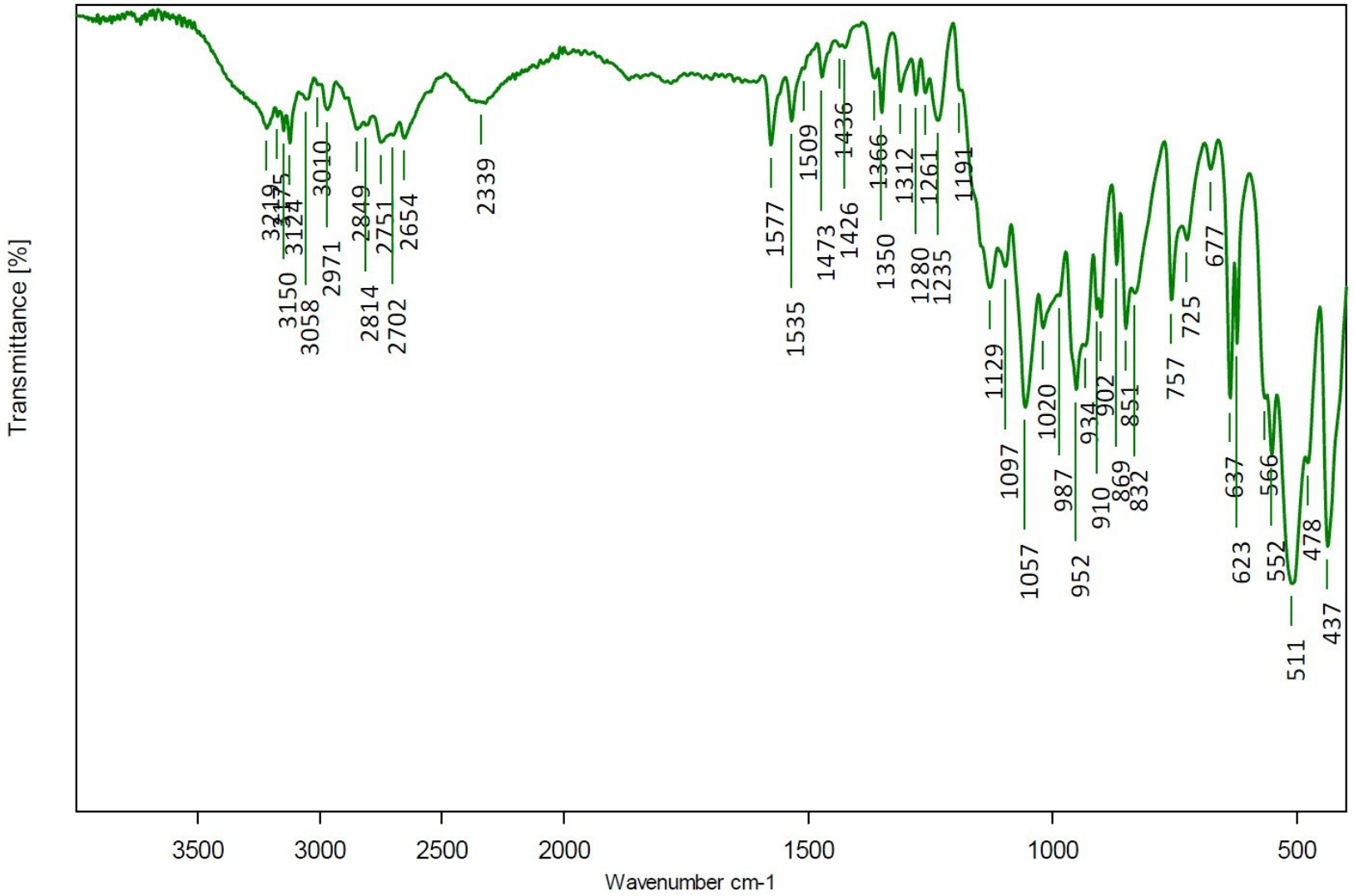

Figure S13. IR spectrum of **1**.

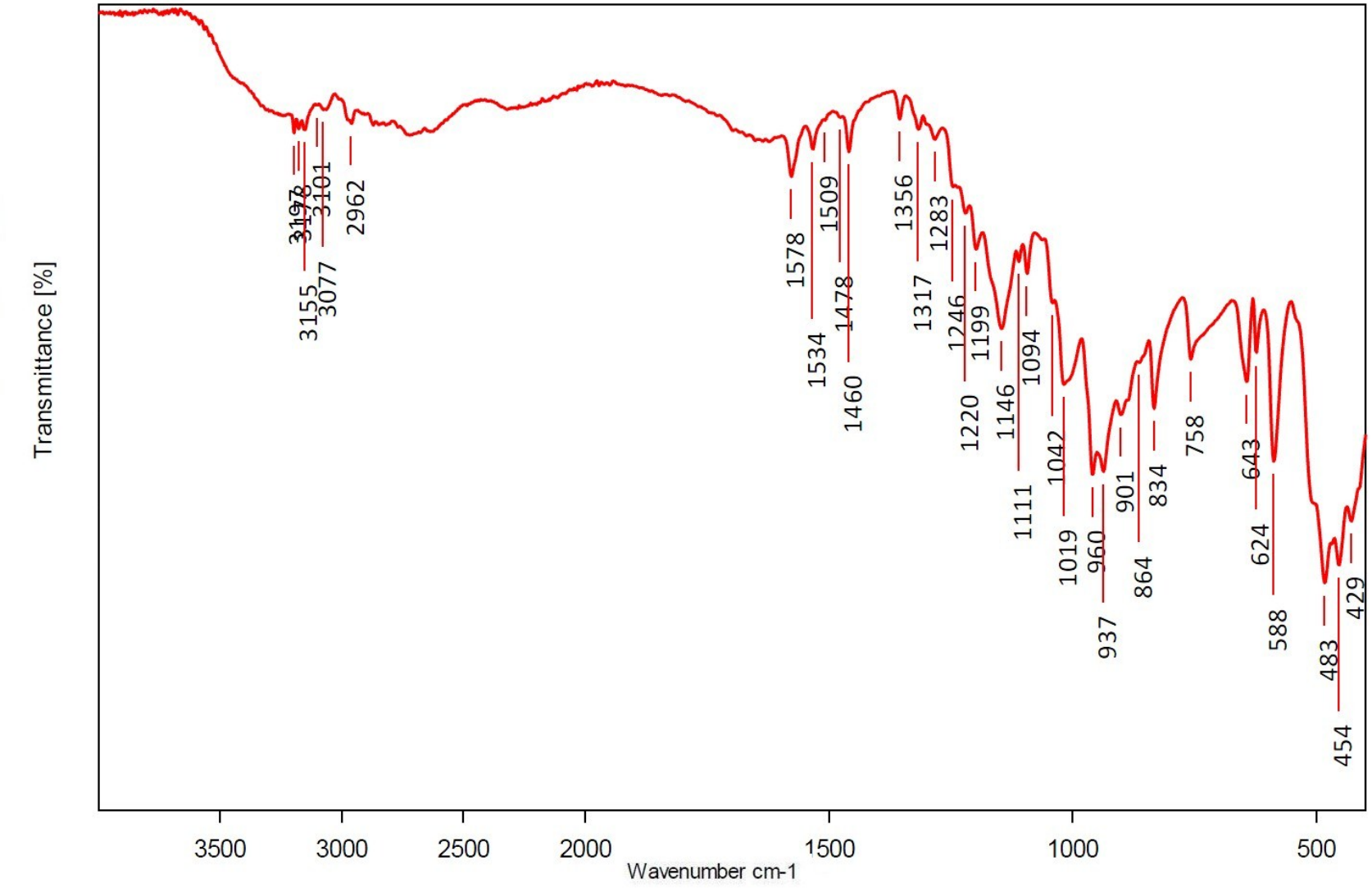

Figure S14. IR spectrum of **2**.

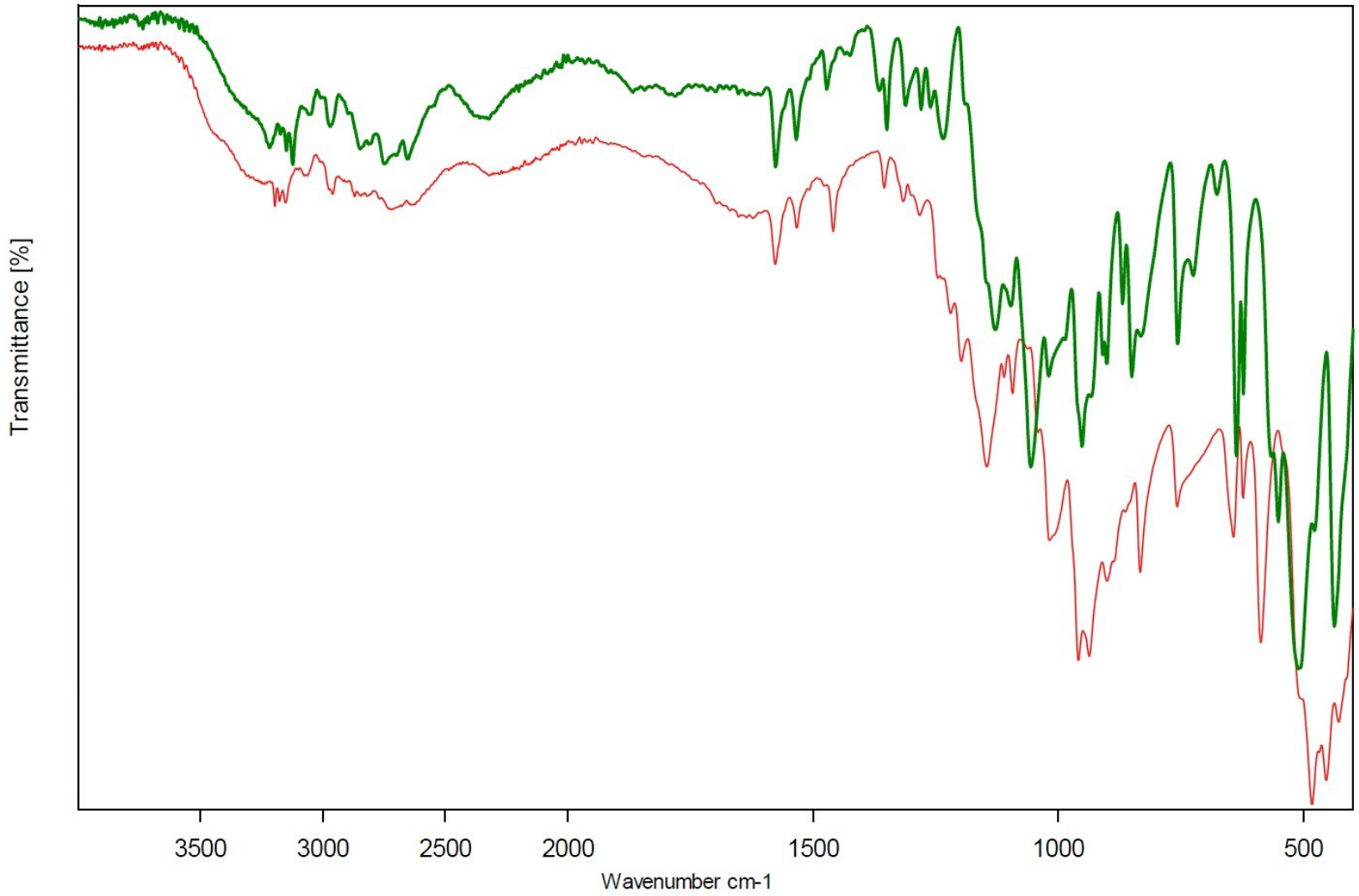

Figure S15. A comparison of IR spectra of ligands **1** (green line) and **2** (red line).

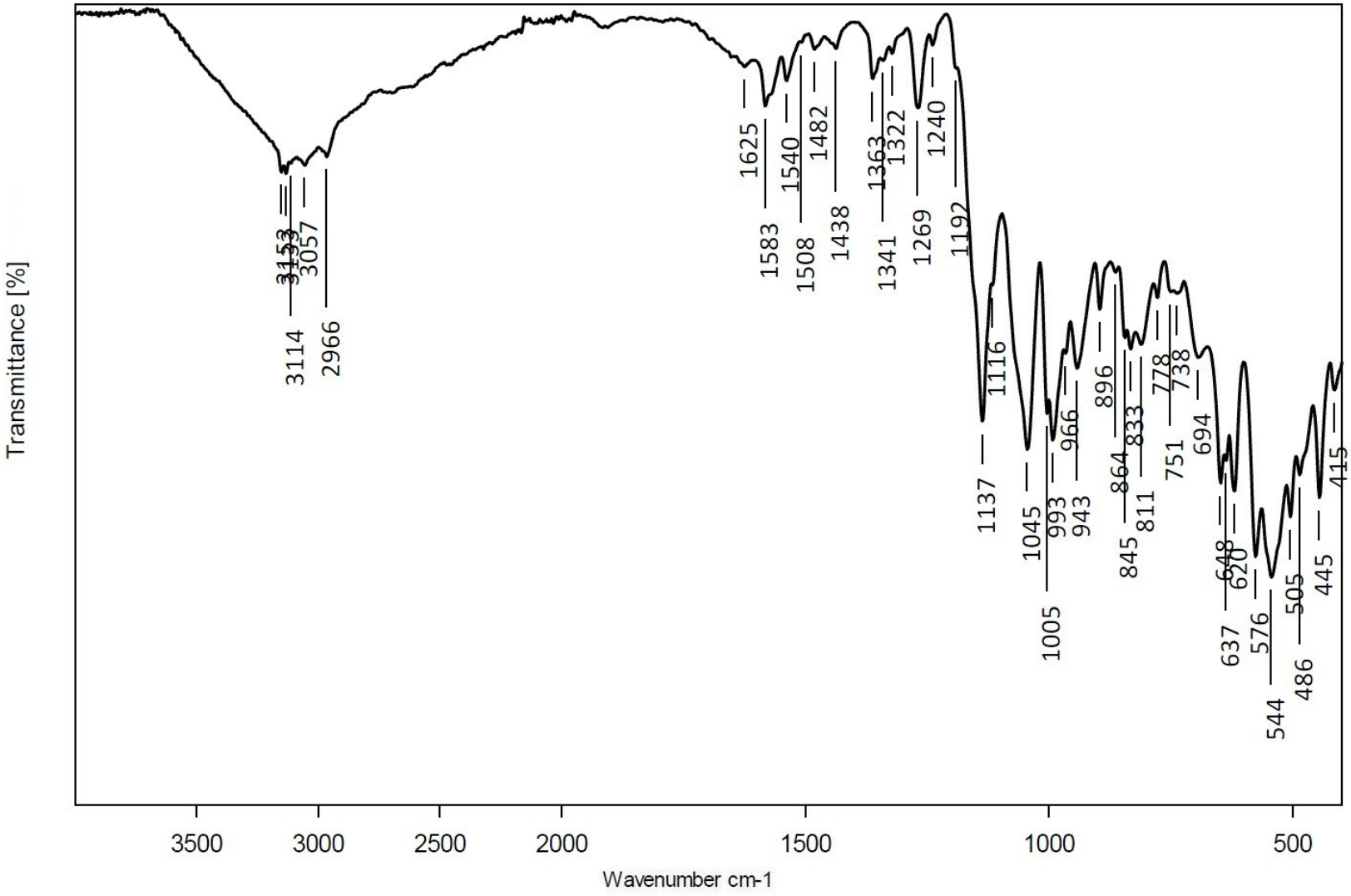

Figure S16. IR spectrum of **1a**.

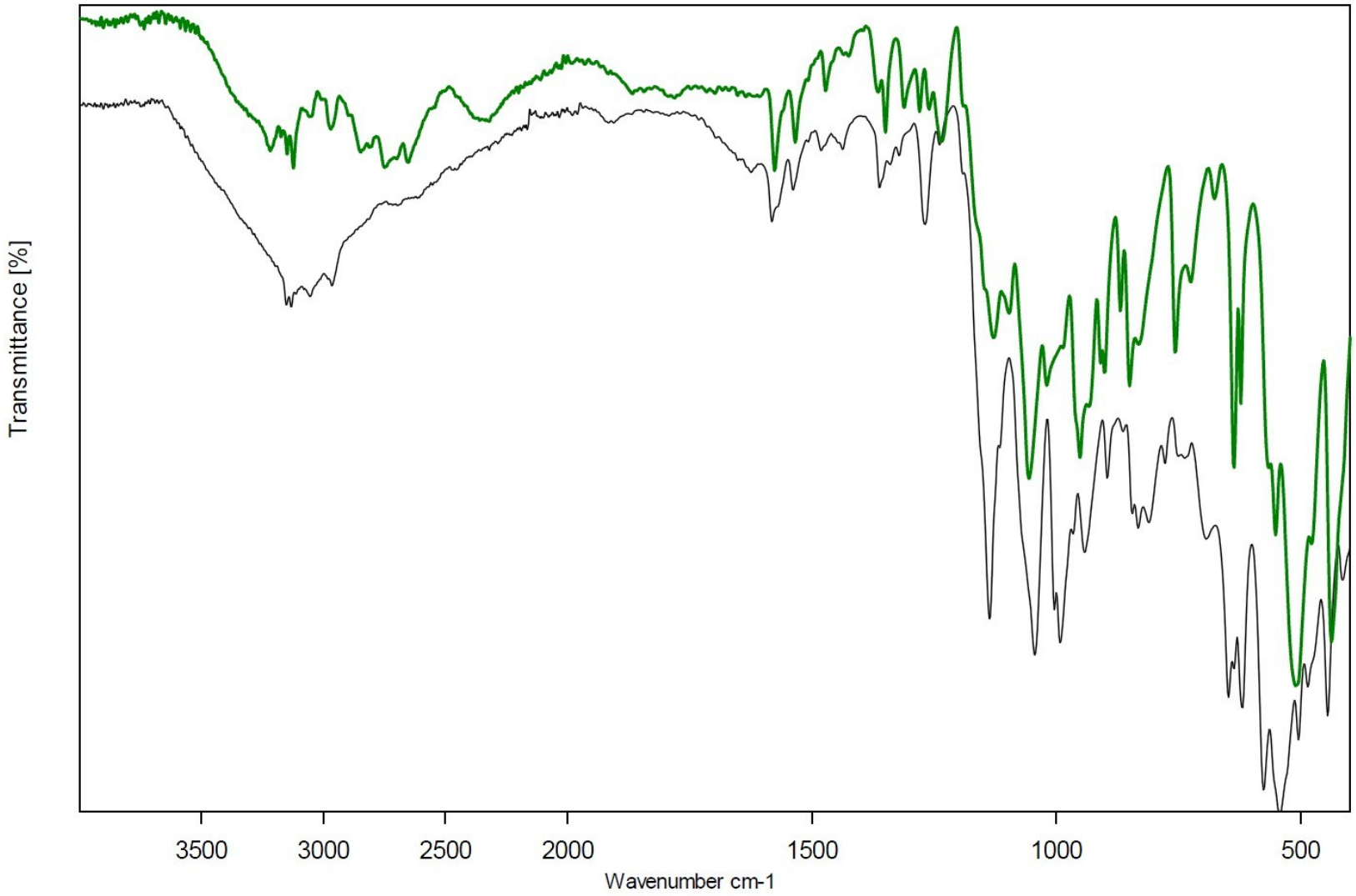

Figure S17. A comparison of IR spectra of ligand **1** (green line) and its coordination polymer **1a** (black line).

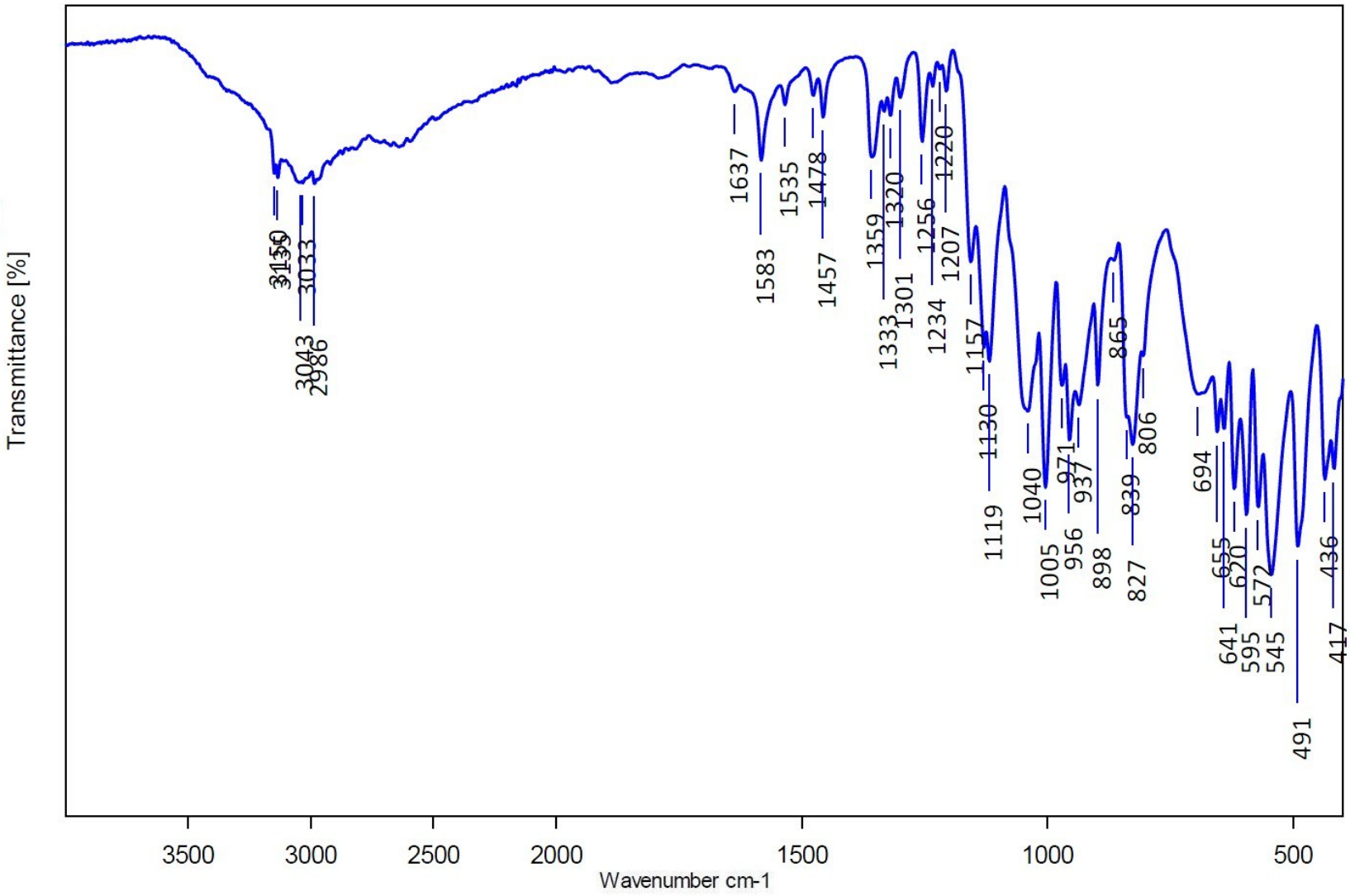

Figure S18. IR spectrum of **2a**.

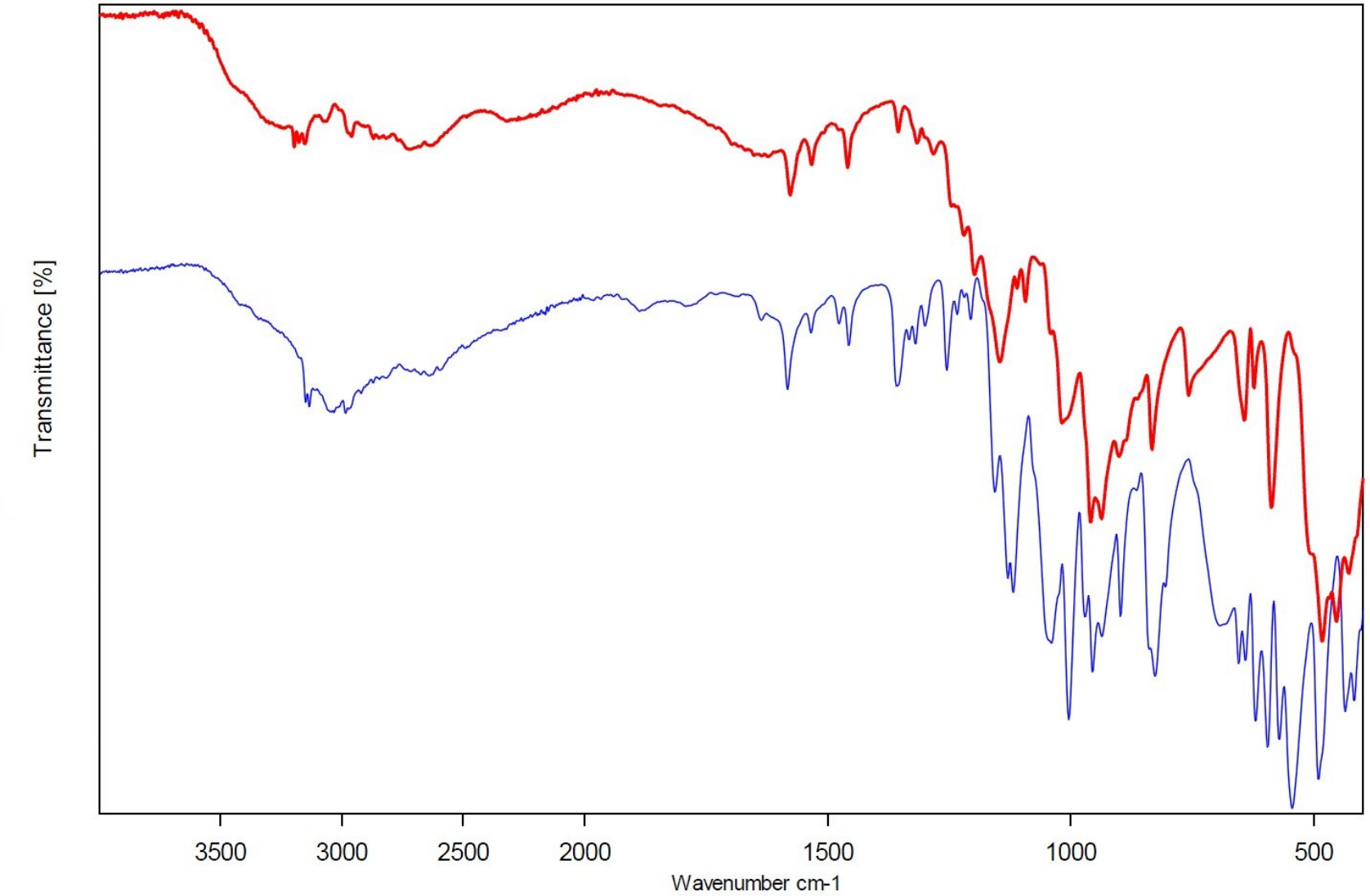

Figure S19. A comparison of IR spectra of ligand **2** (red line) and its coordination polymer **2a** (blue line).

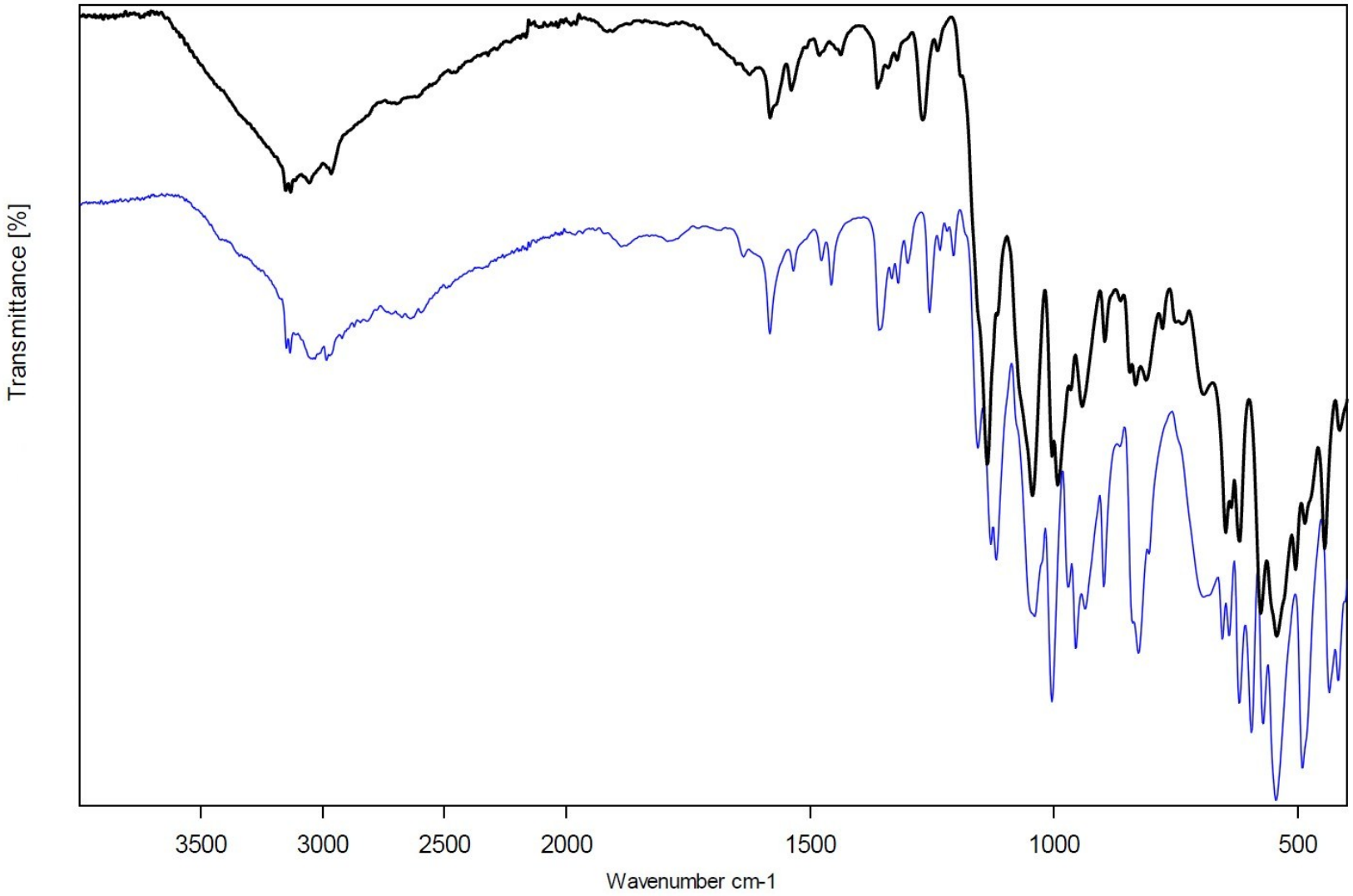

Figure S20. A comparison of IR spectra of coordination polymers **1a** (black line) and **2a** (blue line).

Table S6. Tentative assignments of the observed IR bands [cm^{-1}] for **1**, **2**, **1a** and **2a**.

Wavenumber [cm^{-1}]				*Band assignment*[b]
1	**2**	**1a**	**2a**	
3500-3200 br[a]	3500-3200 br	3500-3200 br	3500-3200 br	ν(O–H) (mostly O–H···O) ν(N–H)/im
3175 3150 3124	3197 3178 3155	3153 3133	3150 3135	ν(C–H)/im
3058 2971	3101 3077 2962	3057 2966	3043 3033 2986	$\nu_{s/as}$(C–H)/CH_2 (cyclobutyl/cyclopentyl ring)
	-	1625	1637	δ(H_2O)
1577	1578	1583	1583	ν(C=C)/im, ν(N=C)/im, ν(N–C)/im δ(C–H)/im
1535	1534	1540	1535	δ(C–H)/im, δ(CO–H)
1509	1509 1478	1508	1478	δ(C–H)/CH_2 (cyclobutyl/cyclopentyl ring)
1473	1460	1482 1438	1457	δ(C–H)/im, δ(N–H)/im
1366 1350 1312 1280 1261 1235 1191	1356 1317 1283 1246 1220 1199	1363 1341 1322 1269 1240 1192	1359 1333 1320 1301 1256 1234 1220 1207	δ(C–H)/im, δ(N–H)/im δ(C–H)/CH_2 (cyclobutyl/cyclopentyl ring)
1129	1146	1137	1157 1130	ν(P=O) δ(PO–H) – in **1** and **2**
-	1111	1116	1119	ν(C–N)/im
1097	1094	-	-	ν(C–OH)
1057 1020	1042 1019	1045 1005 993	1040 1005	ν(P=O) δ(PO–H) – in **1** and **2** δ(CO–H)
987 952 934	960 937	966	971 956 937	δ(C–H)/im, δ(N–H)/im ν(C–C) – cyclobutyl/cyclopentyl ring
910 902	901	896	898	ν(P–O)
869	864	864	865	ν(C–P)
851 832	834	845 833 811	839 827 806	π(im), δ(P–O)
757	758 br	694	694 br	ν(P–O)
725	-	738	-	π(im)
677 637 623 566 552	643 624 588	648 637 620 576 544	655 641 595	π(im), δ(C–C) – cyclobutyl/cyclopentyl ring
511 478 437	483 454 429	505 486 445 415	572 545 491 436 417	δ(O–P–O); δ(C–P)

[a] br – broad; [b] ν_a – antisymmetric stretching; ν_s – symmetric stretching; δ – bending in-plane;π – bending out of plane.

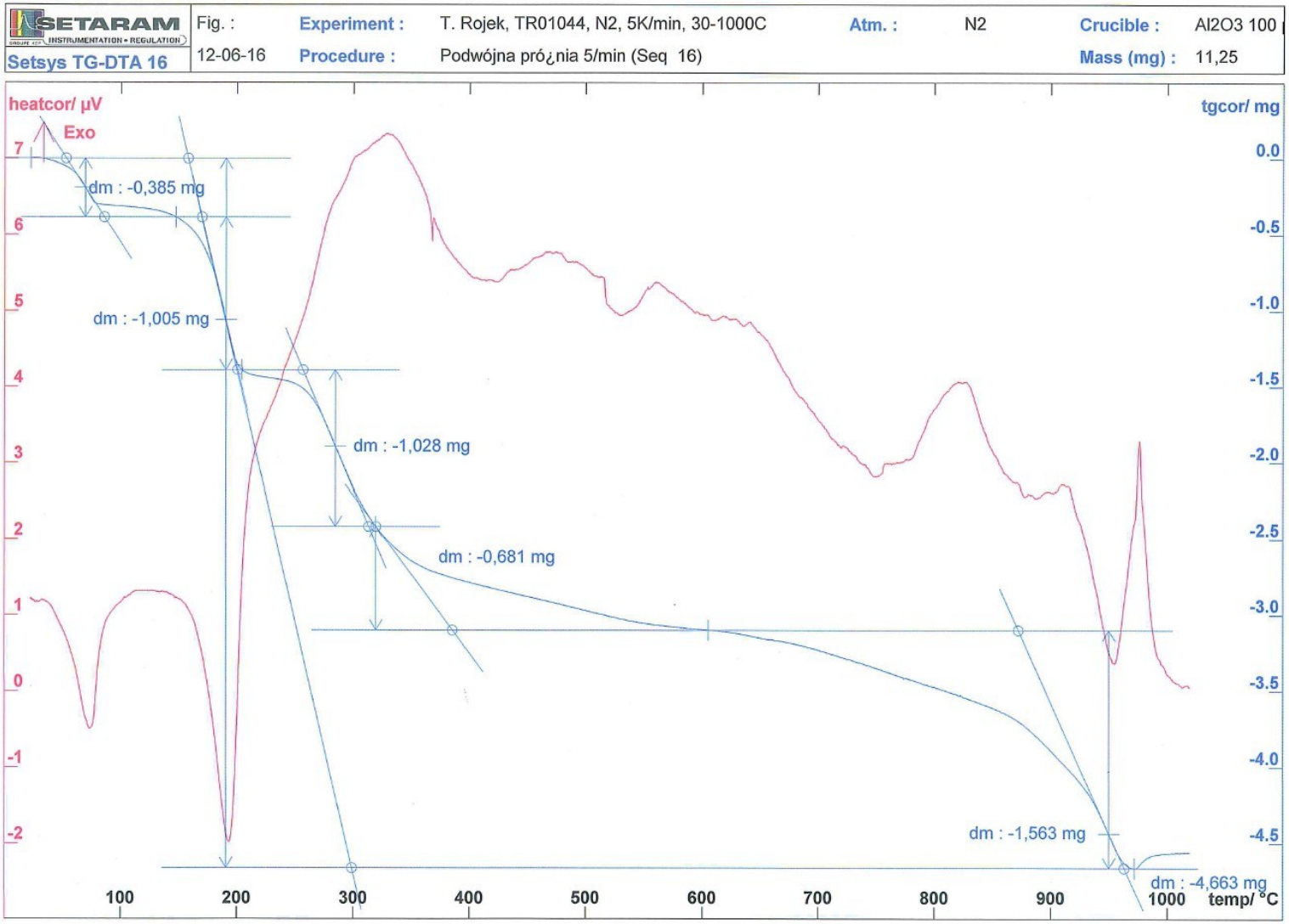

Figure S21. TG-DTA plot for the $Co_3(HcbtZol)_2(H_2O)_6 \cdot 6H_2O$ complex (**1a**).

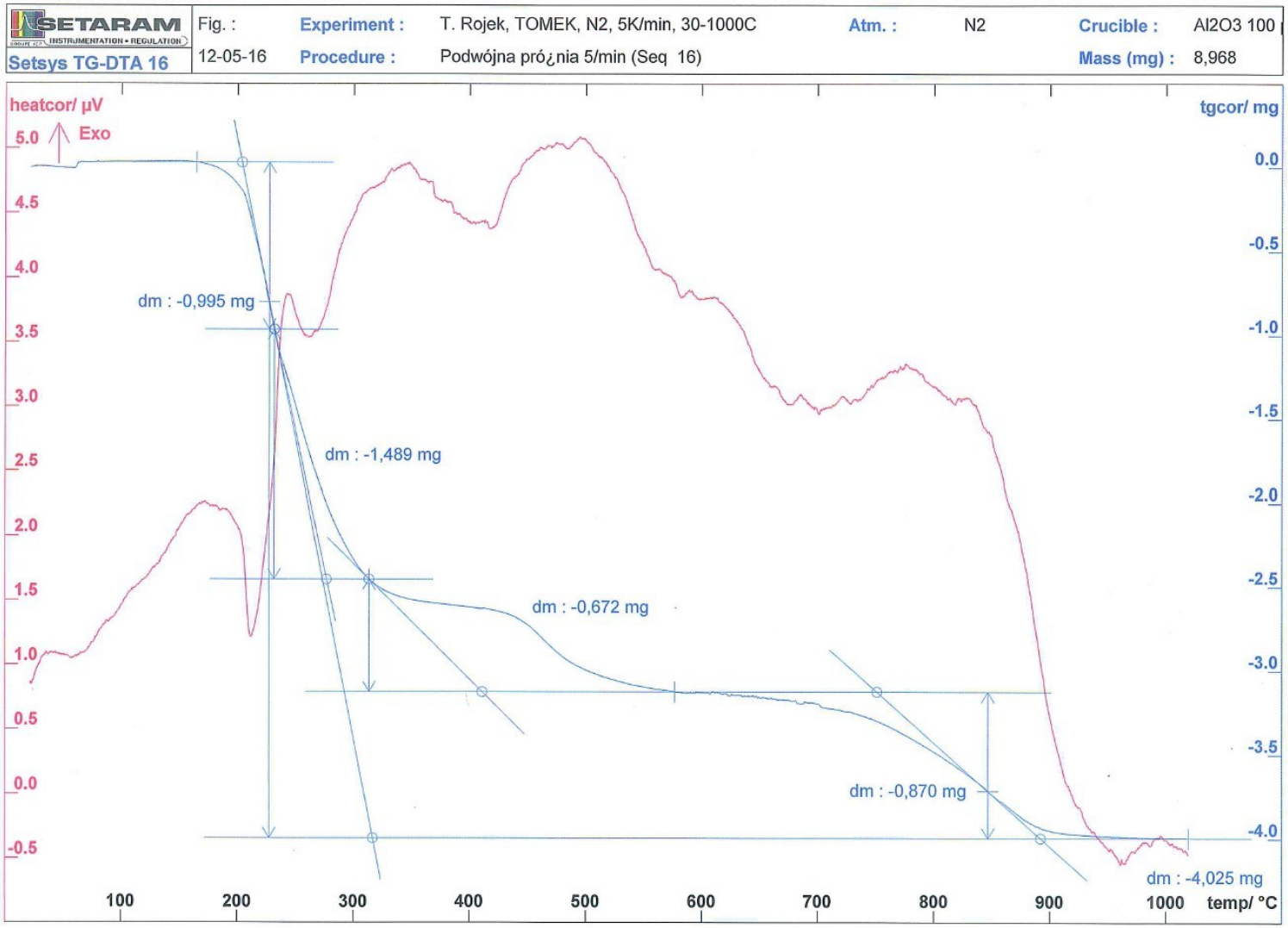

Figure S22. TG-DTA plot for the $Co_3(HcptZol)_2(H_2O)_4 \cdot 2H_2O$ complex (**2a**).

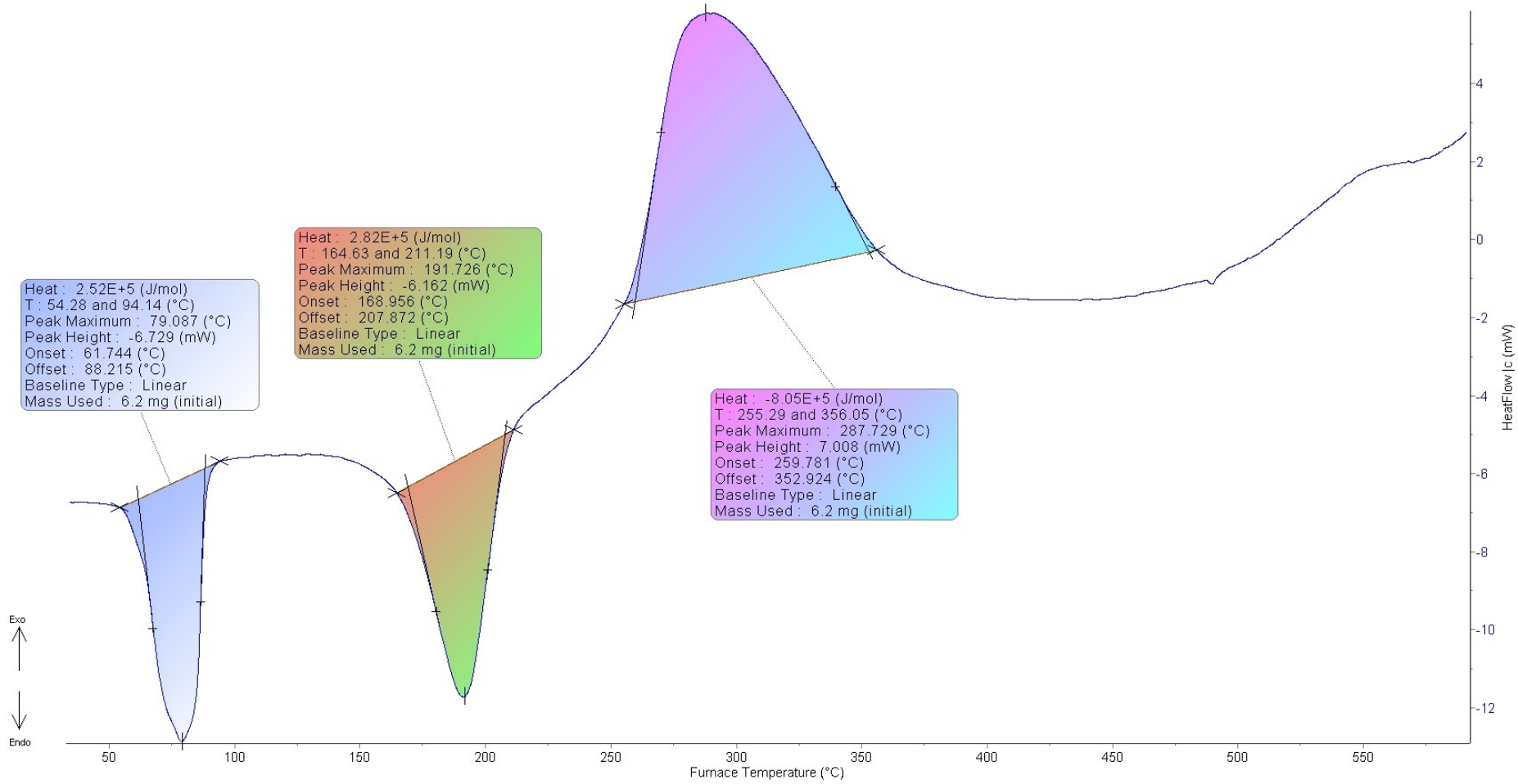

Figure S23. DSC plot for the $Co_3(HcbtZol)_2(H_2O)_6{\cdot}6H_2O$ complex (**1a**).

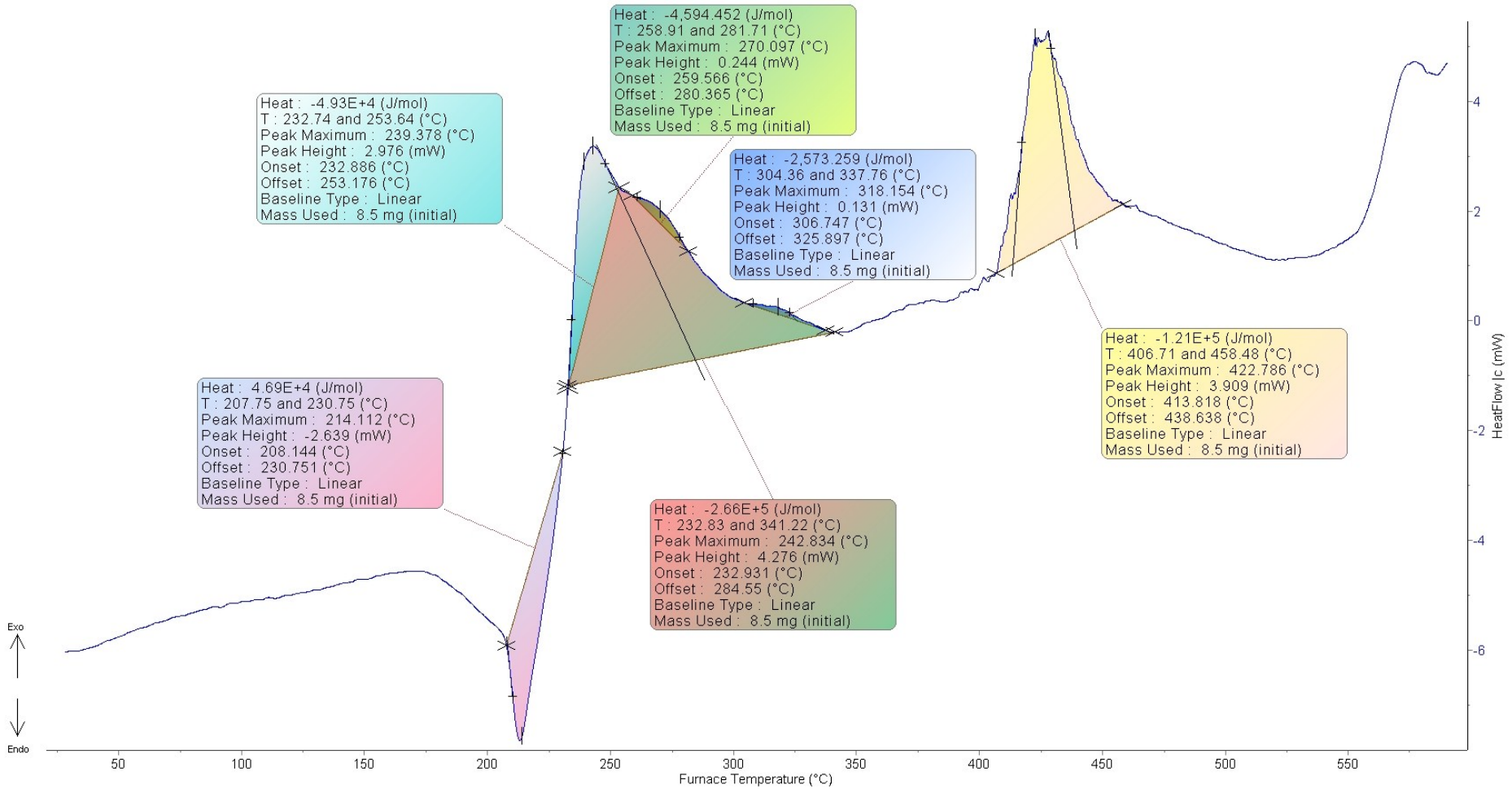

Figure S24. DSC plot for the $Co_3(HcptZol)_2(H_2O)_4 \cdot 2H_2O$ complex (**2a**).

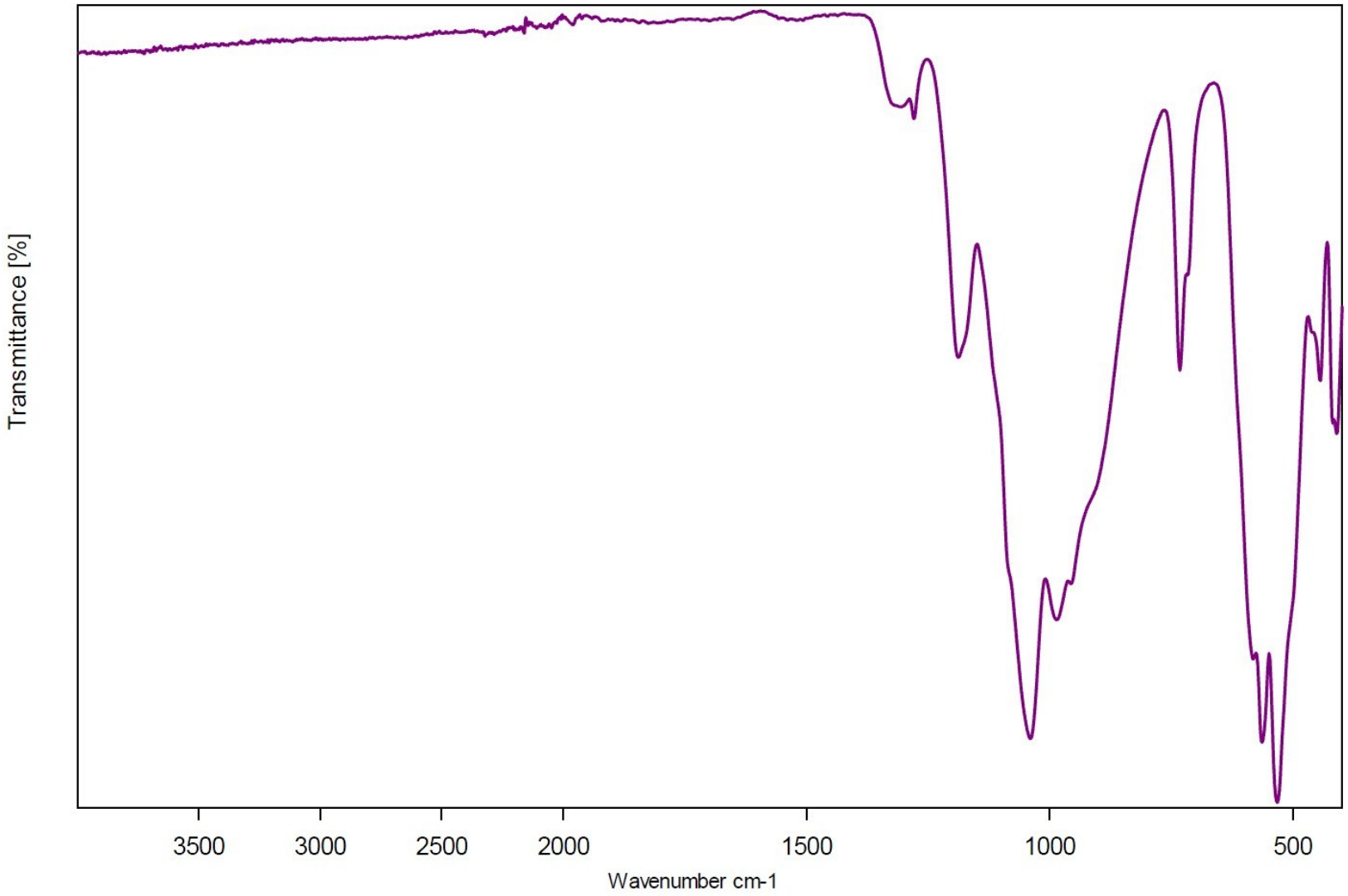

Figure S25. IR spectrum of solid residue, obtained by heating a crystalline sample of **1a** up to 1000 °C.

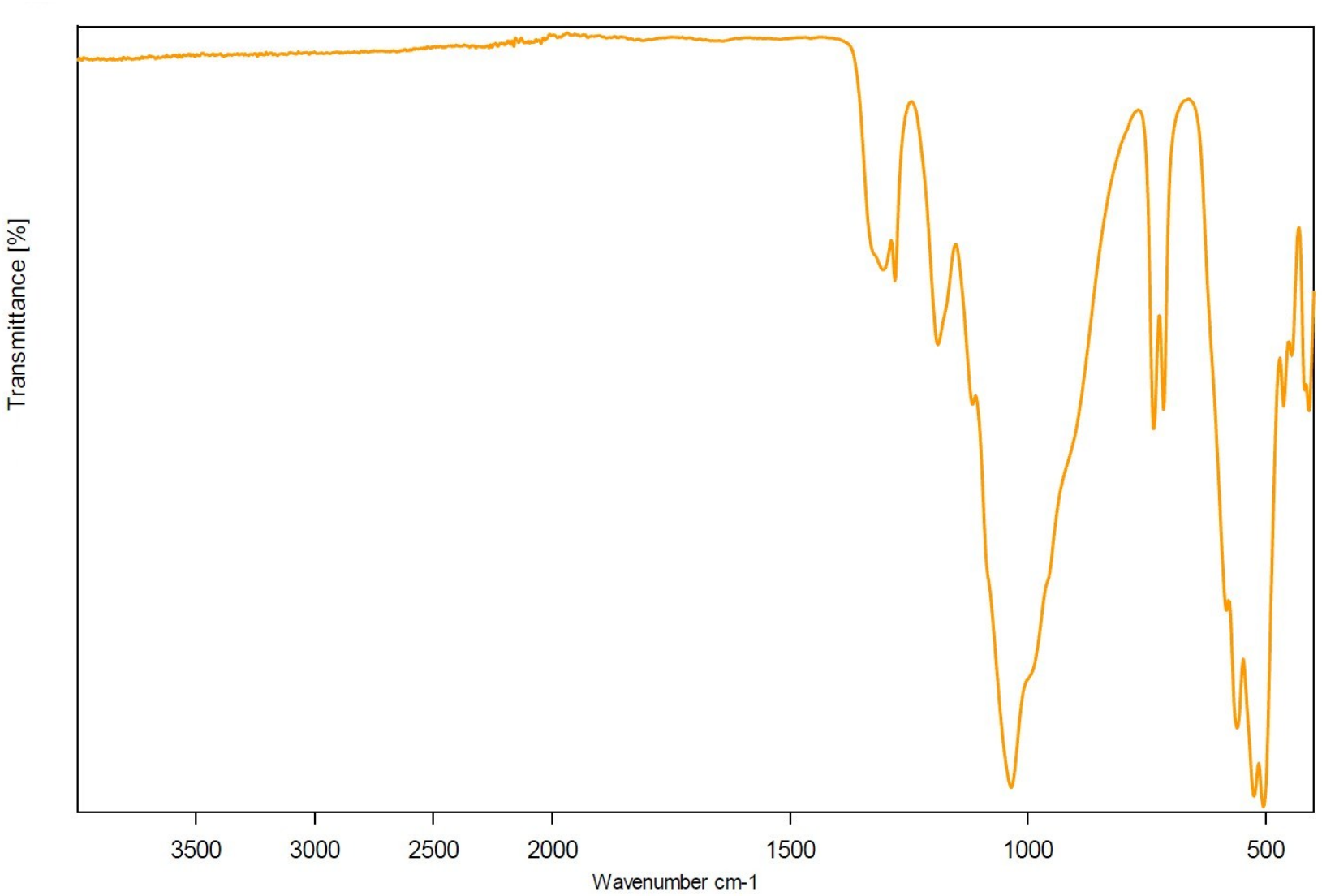

Figure S26. IR spectrum of solid residue, obtained by heating a crystalline sample of **2a** up to 1000 °C.

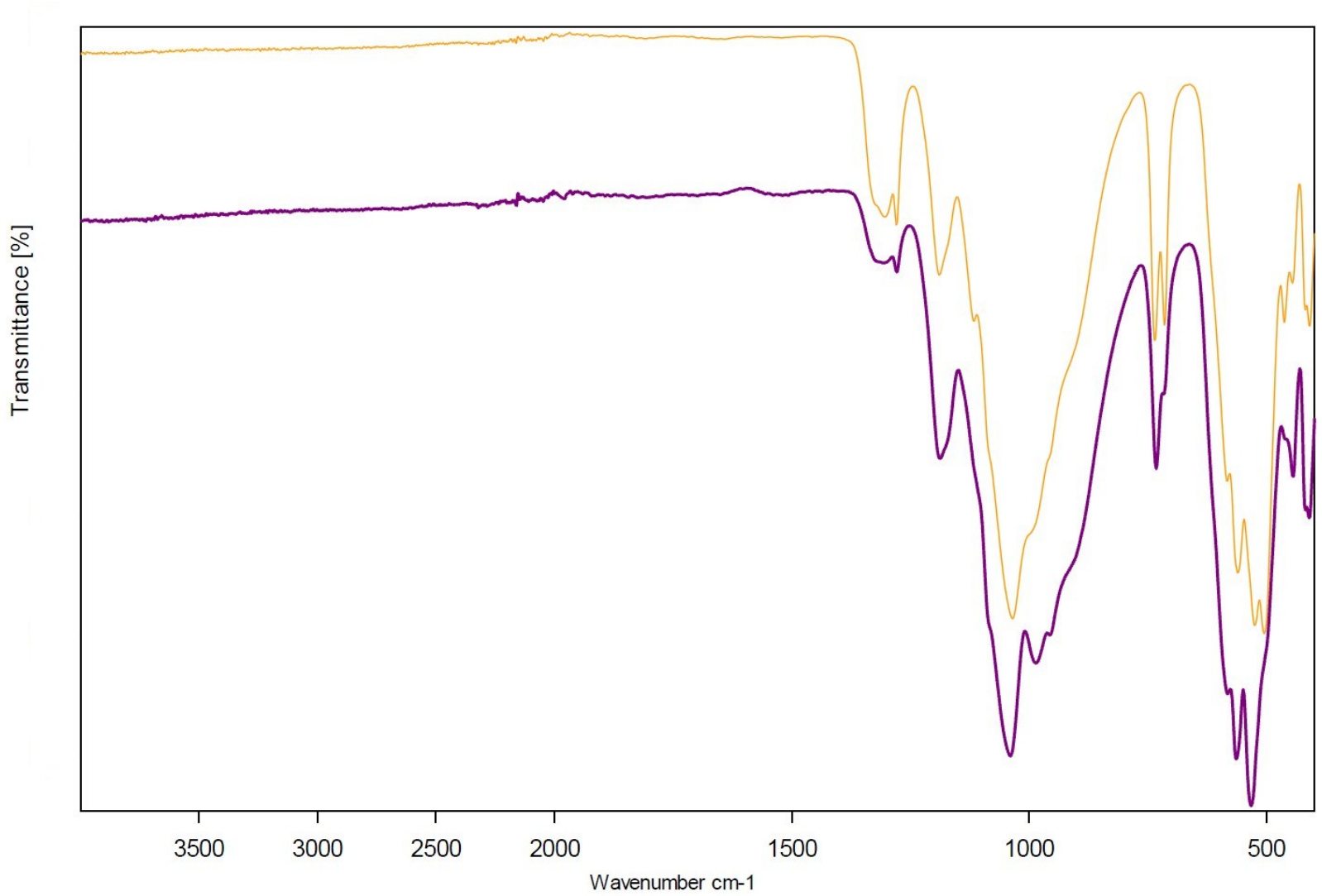

Figure S27. A comparison of IR spectra of solid residues, obtained by heating a crystalline sample of **1a** (purple line) and **2a** (orange line) up to 1000 °C.

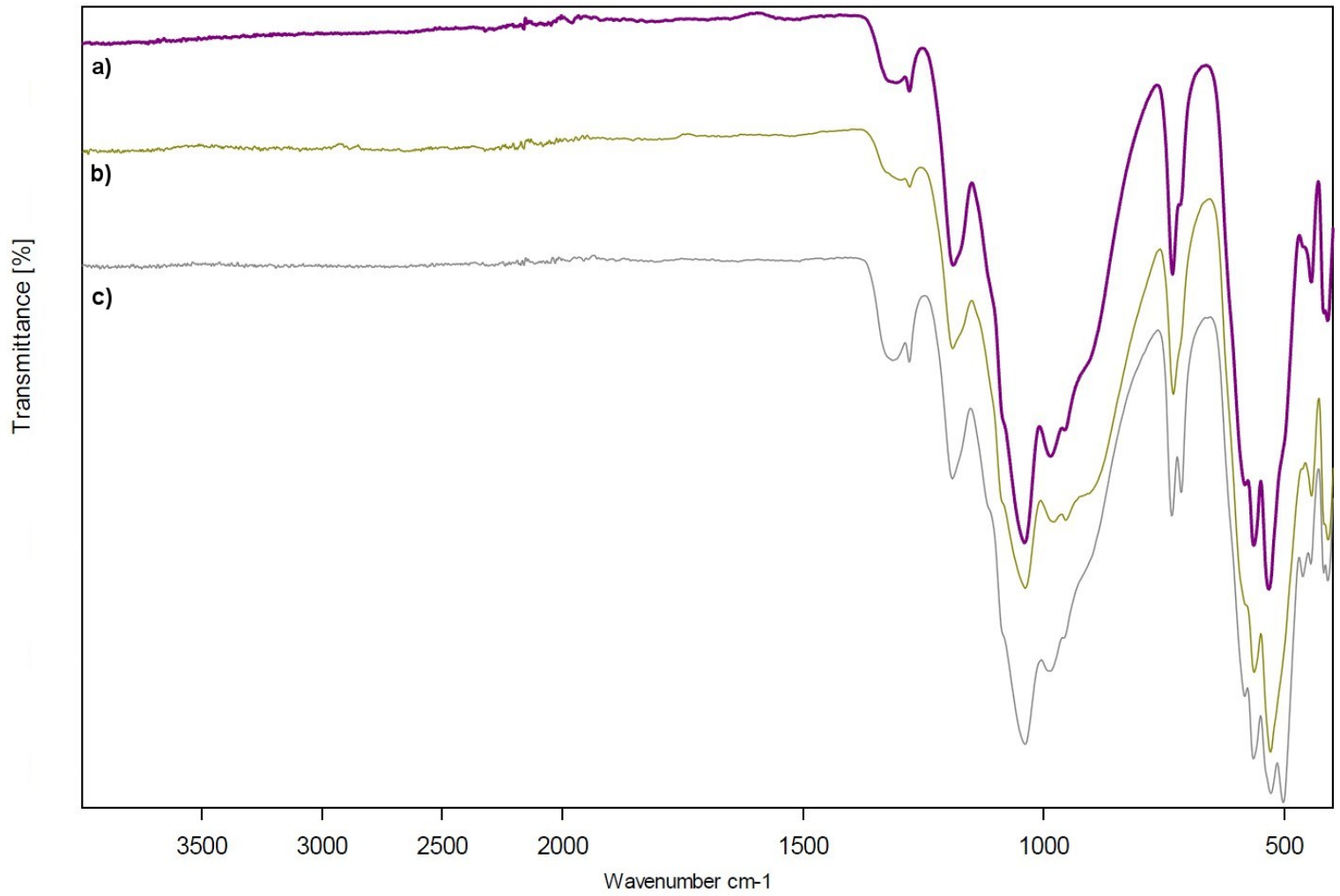

Figure S28. A comparison of IR spectra of solid residues, obtained by heating a crystalline sample of (a) **1a**, (b) Co(II) complex of dimethyl substituted analog of zoledronic acid – $Co_3(HdmtZol)_2(H_2O)_6{\cdot}6H_2O$ and (c) cyclopropane substituted analog of zoledronic acid – $Co_3(HcppZol)_2(H_2O)_6{\cdot}6H_2O$ up to 1000 °C.

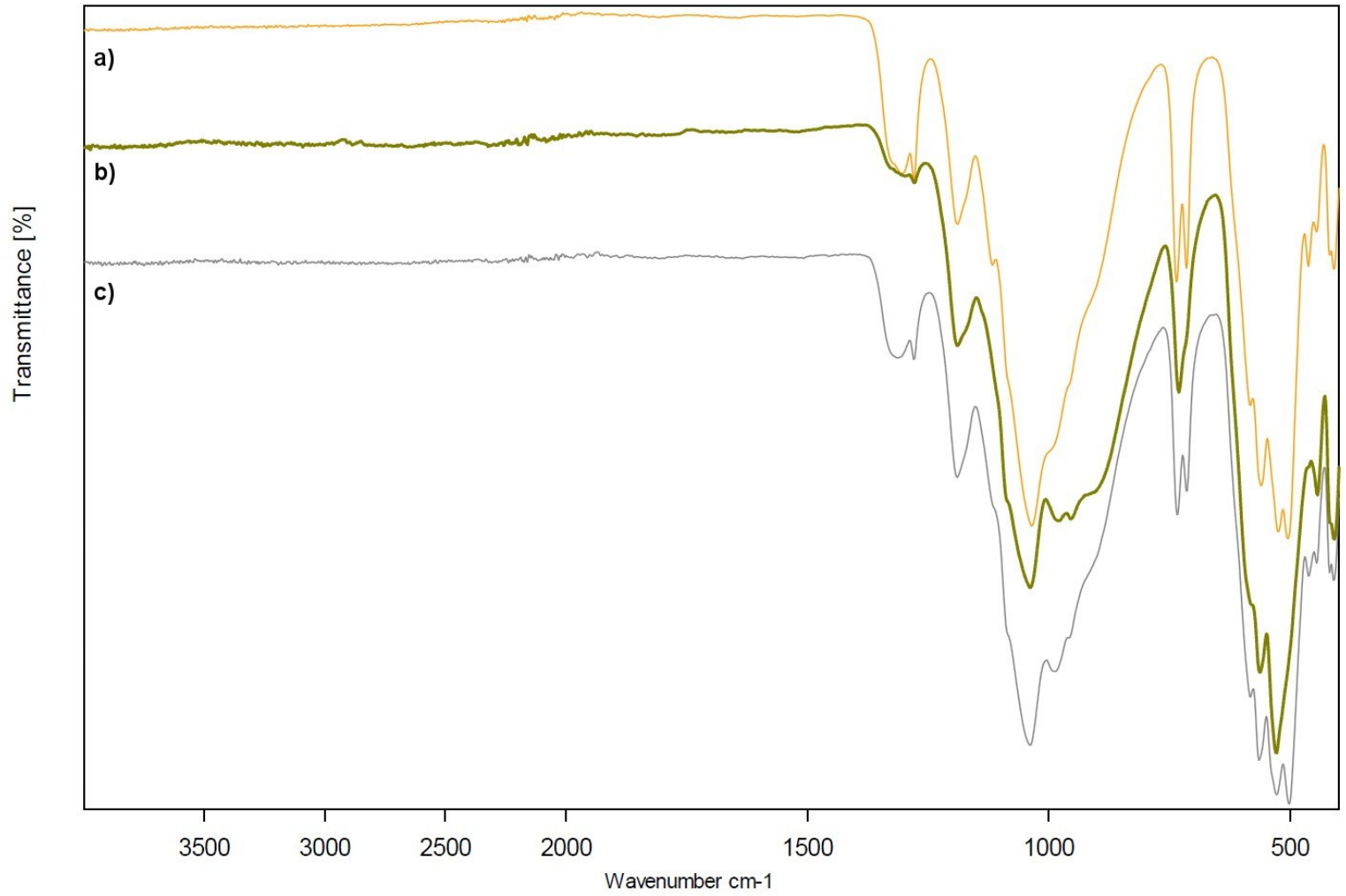

Figure S29. A comparison of IR spectra of solid residues, obtained by heating a crystalline sample of (a) **2a**, (b) Co(II) complex of dimethyl substituted analog of zoledronic acid – $Co_3(HdmtZol)_2(H_2O)_6{\cdot}6H_2O$ and (c) cyclopropane substituted analog of zoledronic acid – $Co_3(HcppZol)_2(H_2O)_6{\cdot}6H_2O$ up to 1000 °C.

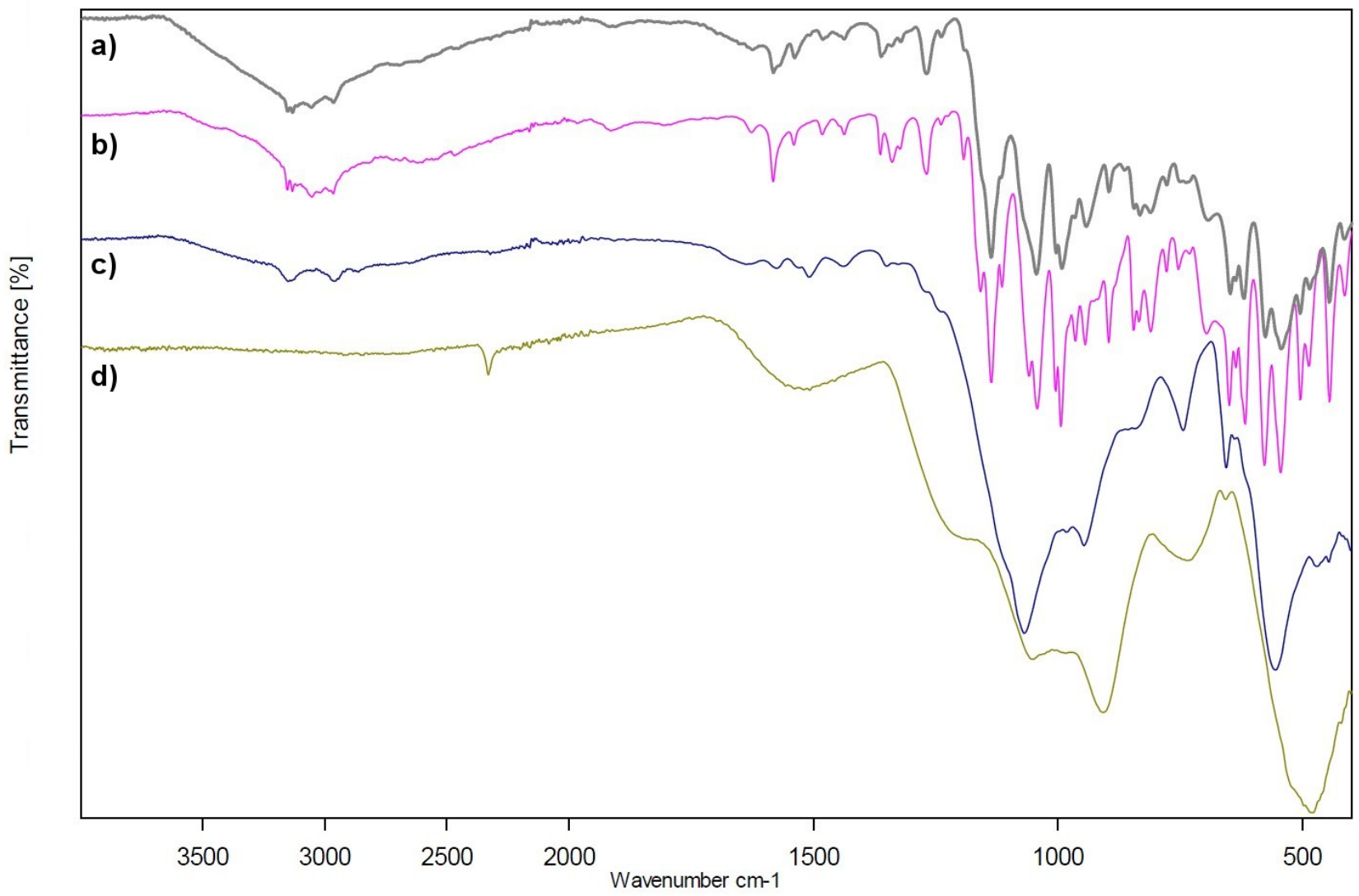

Figure S30. IR spectra of (a) crystalline **1a** and solids obtained by heating sample of the complex up to (b) 120 °C; (c) 210 °C; (d) 600 °C.

a)

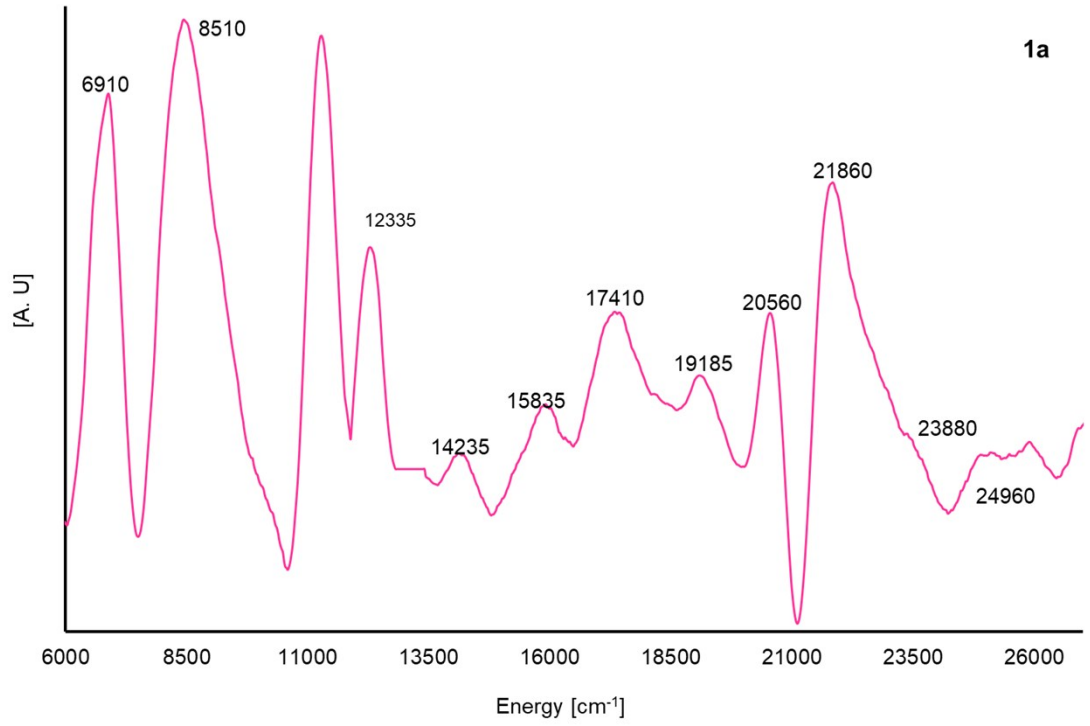

b)

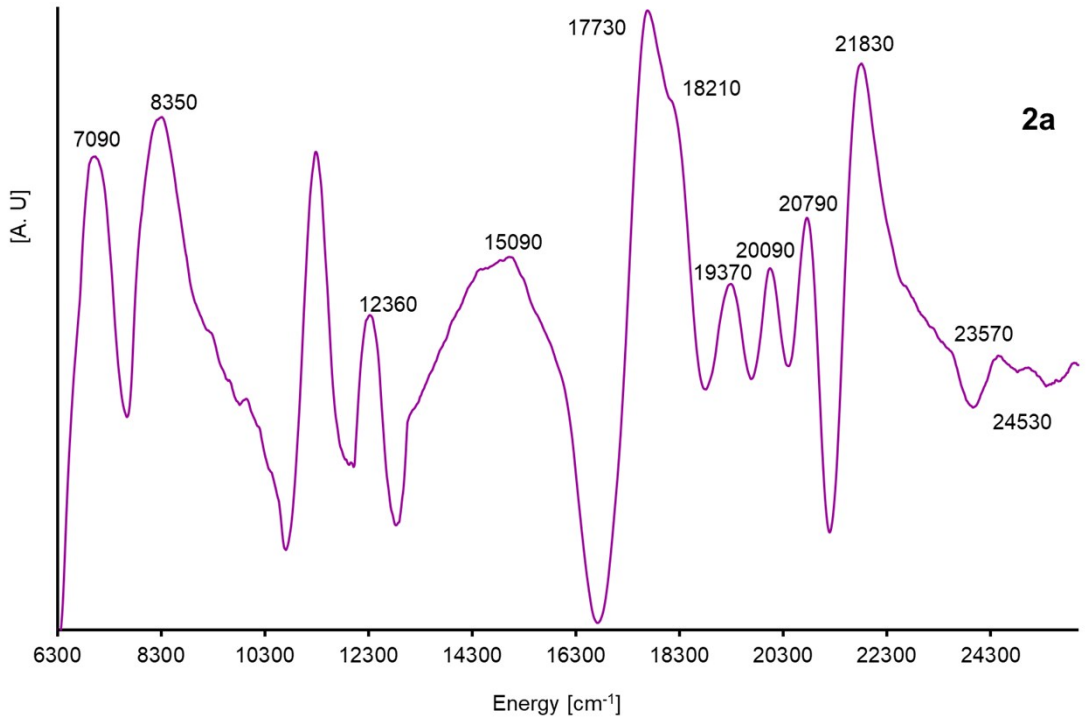

Figure S31. The effect of filtering process of the diffuse-reflectance spectra of the compounds (a) **1a** and (b) **2a** in the spectral range from 6000 cm^{-1} to 26000 cm^{-1}.

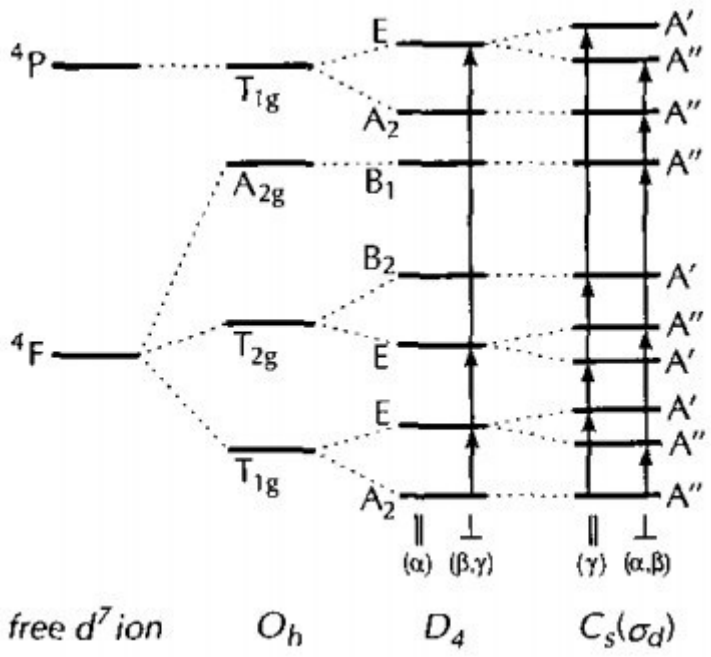

Scheme S1. The crystal field splitting diagram and symmetryselectionrules for cobalt(II) ions (d^7configuration, quartetstates) [26].

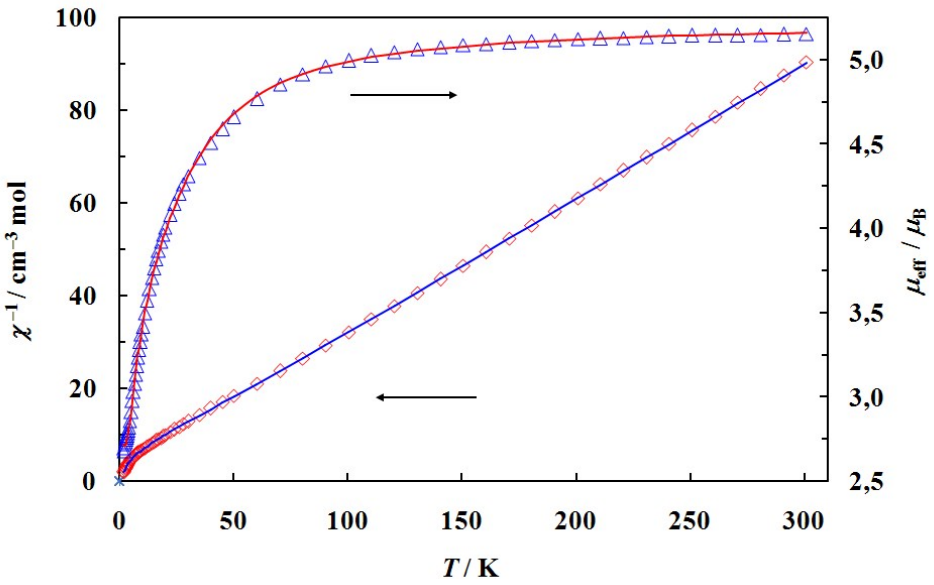

Figure S32. Temperature dependence of the effective magnetic moments of **1a** (triangles) and the reciprocal magnetic susceptibility (diamonds). The solid lines show the best fit of the data according to model **C**.

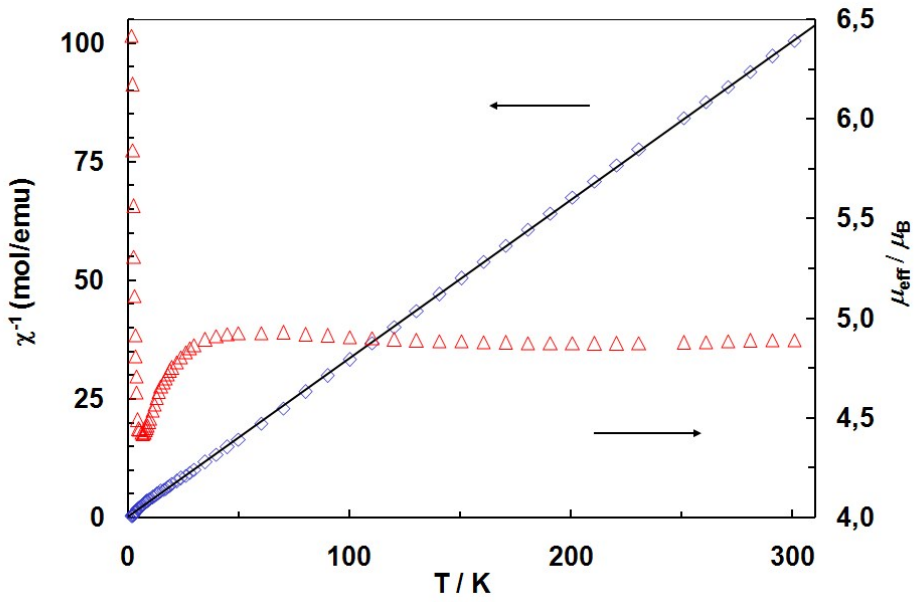

Figure S33. Temperature dependence of the effective magnetic moments of **2a** (triangles) and the reciprocal magnetic susceptibility (diamonds). The solid lines show the fit to the Curie-Weiss law (130-300 K).

Table S7. The results of fitting procedure for **2a** with fixed $J_1 + J_3 = 8.64$ cm^{-1}(Ising distorted diamond chain).

J_1 (cm^{-1})#	-1.00	-2.00	-3.00	-4.00	-5.00	-6.00	-7.00	-8.00
J_2 (cm^{-1})#	-7.64	-6.64	-5.64	-4.64	-3.64	-2.64	-1.64	-0.64
J_3 (cm^{-1})	17.33	16.35	15.78	15.55	15.60	15.94	16.65	17.78
g	5.68	5.70	5.70	5.70	5.70	5.70	5.69	5.68
TIP#	6.70E-05	6.70E-05	6.70E-05	6.70E-05	6.70E-05	6.70E-05	6.70E-05	6.70E-05
zJ'	-2.94	-2.97	-2.99	-3.00	-2.99	-2.98	-2.96	-2.92
R	1.40E-04	1.20E-04	1.11E-04	1.08E-04	1.09E-04	1.13E-04	1.25E-04	1.50E-04

#fixedvalues